Short title: Ketocarotenoid Synthesis and Sequestration

Corresponding author:

Paul D. Fraser
School of Biological Sciences,
Royal Holloway University of London,
Egham Hill, Egham, Surrey,
TW20 0EX.
UK.

Phone; +44 (0)1784 443894

Email: p.fraser@royalholloway.ac.uk

The formation and sequestration of non-endogenous ketocarotenoids in transgenic *Nicotiana glauca*

Cara L. Mortimer[a,1], Norihiko Misawa[b], Laura Perez-Fons[a], Francesca P. Robertson[a] Hisashi Harada[b], Peter M. Bramley[a] and Paul D. Fraser[a,2]

[a]School of Biological Sciences, Royal Holloway University of London, Egham, Surrey, TW20 0EX, UK
[b]Research Institute for Bioresources and Biotechnology, Ishikawa Prefectural University, Suematsu, Nonoichi-machi, Ishikawa, 921-8836, Japan

[1]Current address: Centre for Tropical Crops and Biocommodities, Queensland University of Technology, Brisbane, QLD 4001, Australia.

Summary: The study illustrates the production of ketocarotenoids in *Nicotiana glauca*, the adaptation of the plastid to sequester non-endogenous carotenoids and the robustness of plant metabolism to these changes.

Author contributions: PDF, PMB and CLM conceived the original screening and research plans;PDF and PMB supervised the experiemnts;CLM performed most of the experiments; HH and NM provided vital materials. LP performed MS analysis of the carotenoids; FPR carried out MS analysis of proteins/peptides; PDF and CLM designed the experiments and analysed the data; PDF, CLM and PMB conceived the project; PDF and CLM wrote the article with contributions of all authors. PDF and PMB acquired the funding.

Financial support: N.M. and H.H. are grateful for support from the New Energy and Industrial Technology Development Organization (NEDO), Japan. The study was also funded by the European Commission FP6-2005-FOOD-4B programme, grant # 036296 to P.D.F and P.M.B, The European Union Framework Program 7 METAPRO and MultiBioPro (244348 and 311804) funded under the Knowledge-Based Bio-Economy program to P.D.F.

Present addresses: [1]CLM current address is Centre for Tropical Crops and Biocommodities, Queensland University of Technology, Brisbane, QLD 4001, Australia.

[2]Address correspondence to p.fraser@royalholloway.ac.uk

The author responsible for distribution of materials to the findings presented in this article in accordance with the policy described in the Instructions for Authors (www.plantphysiol.org) is Paul D. Fraser (p.fraser@royalholloway.ac.uk).

ABSTRACT

Ketolated and hydroxylated carotenoids are high-value compounds with industrial, food and feed applications. Chemical synthesis is presently the production method of choice for these compounds, with no amenable plant sources readily available. In the present study, the 4, 4' β-oxygenase (*crtW*) and 3, 3' β-hydroxylase (c*rtZ*) genes from *Brevundimonas* sp SD-212. have been expressed under constitutive transcriptional control in *Nicotiana glauca*, which has an emerging potential as biofuel and biorefining feedstock. The transgenic lines produced significant levels of non-endogenous carotenoids in all tissues. In leaf and flower the carotenoids (ca. 0.5% dry weight) included 0.3 and 0.48 %, respectively, of non-endogenous keto and hydroxylated carotenoids. These were 4-ketolutein, echinenone (and its 3-hydroxy derivatives), canthaxanthin, phoenicoxanthin, 4-ketozeaxanthin and astaxanthin. Stable, homozygous genotypes expressing both transgenes, inherited the chemotype. Subcellular fractionation of vegetative tissues and microscopic analysis revealed the presence of ketocarotenoids in thylakoid membranes, not predominantly in the photosynthetic complexes, but in plastoglobules. Despite ketocarotenoid production and changes in cellular ultrastructure, intermediary metabolite levels were not dramatically affected. The study illustrates the utility of *Brevundimonas* CRTZ and W to produce ketocarotenoids in a plant species that is being evaluated as a biorefining feedstock, the adaptation of the plastid to sequester non-endogenous carotenoids and the robustness of plant metabolism to these changes.

INTRODUCTION

Sustainable development is at the forefront of the 21st century's agenda. To achieve this goal, innovative approaches must be developed to switch from existing, chemically based non-renewable sources to biological raw materials. Ketocarotenoids, such as canthaxanthin and astaxanthin, are examples of high value pigments used in the food, feed and health sectors (Breithaupt, 2007), which are presently produced by chemical synthesis, using precursors derived from the petrochemical industry (Ausich, 1997).

Several algal species can act as natural sources, but production requires high light, controlled nutrient depletion and extended growth periods, which increase susceptibility to contamination (Lorenz and Cysewski, 2000). With the exception of several marine bacteria (Misawa et al., 1995) and the fungus *Xanthophyllomyces dendrorhous* (Park et al., 2009), microbes capable of synthesising ketocarotenoids are rare. On a hectare basis, higher plant sources are the most economically favourable (Ausich, 1997) and offer the least environmental impact. Unfortunately, *in planta*, the presence of ketocarotenoids, such as astaxanthin, has only been reported in the flowers of the *Adonis* species (Cunningham and Gantt, 2005). This plant is not readily amenable to agricultural production. Although *Adonis* and microbial sources may not be suitable production hosts, their biosynthetic genes have been isolated, facilitating metabolic engineering in heterologous hosts. Ketocarotenoid formation has been engineered into a number of crop plants, giving rise to a myriad of keto/hydroxylated carotenoids, with varying qualitative and quantitative profiles. For example maize (*Zea mays;*(Zhu et al., 2008), potato (*Solanum phureja* and *Solanum tuberosum*; (Gerjets and Sandmann, 2006; Morris et al., 2006), tomato (*Solanum lycopersicum*; (Huang et al., 2013), carrot (*Daucus carota*; (Jayaraj et al., 2008), rapeseed (*Brassica napus*; (Fujisawa et al., 2009), lettuce (*Lactuca sativa*; Harada et al., 2014), and tobacco (*Nicotiana tabacum*; (Hasunuma et al., 2008). In the present study, the 4, 4' carotenoid oxygenase (*crtW*) and

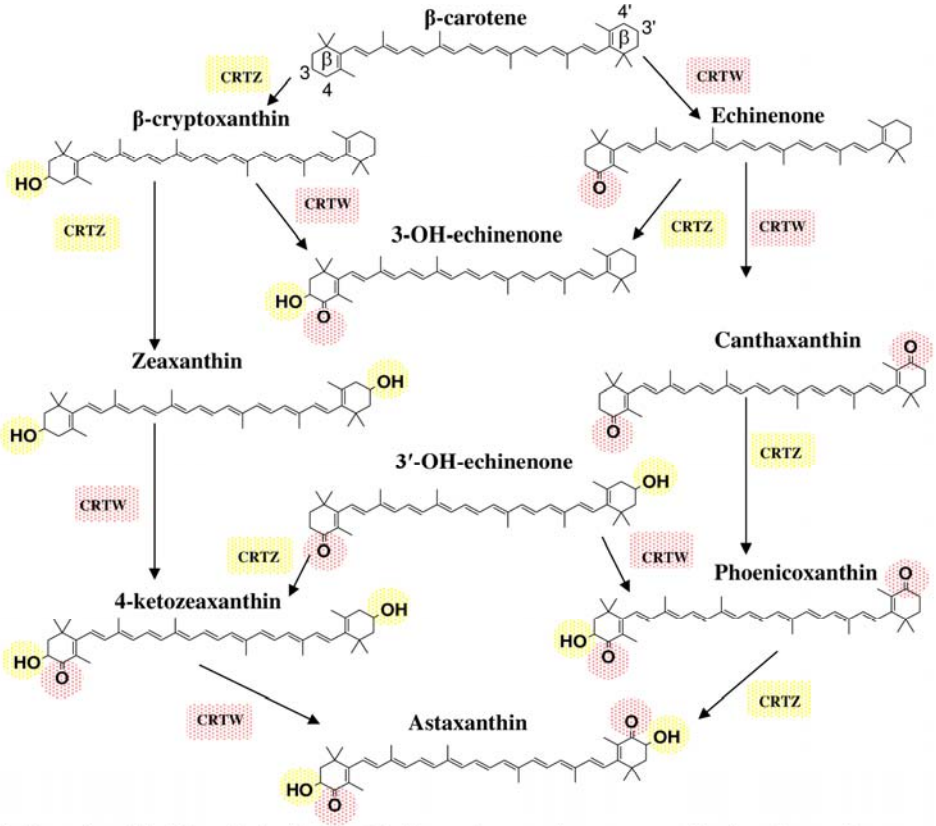

Figure 1. Schematic illustration of the biosynthesis of astaxanthin from endogenous β-carotene, resulting from *Brevundimonas* sp. *crtW* and *crtZ* expression in *N. glauca* plants. Enzymes are indicated by their gene assignment symbols: CRTW, β-carotene ketolase; CRTZ, 3,3` hydroxylase coloured shading also indicates the functional groups introduced by these enzymes.

3, 3' carotenoid hydroxylase (*crtZ*) genes from *Brevundimonas* (Choi et al., 2005; 2006; 2007) have been utilized to convert endogenous carotenoids such as β-carotene and zeaxanthin to a diverse array of keto/hydroxyl carotenoid products/precursors (Fig. 1). The composition of the different carotenoids formed typically reflects the enzymatic properties and promiscuity of the individual enzymes (Fraser et al., 1998). For example, the CRTZ enzymes from bacteria are less efficient at introducing keto moieties after the β-rings have been hydroxylated at the 3, 3' position (Fraser et al., 1998). β–carotene and zeaxanthin are the precursors used by these enzymes in their native organisms. However, the ability of the enzymes to act on other plant based carotenoids cannot be ruled out and is an objective of the study. CRTW is capable of introducing keto groups at the 4 and 4' positions of the carotenoid β-ionone rings, in the absence or presence of hydroxylation at the 3, 3' position (Fig. 1). Thus, CRTW can act directly on endogenous β-carotene or zeaxanthin as precursors. CRTZ from *Brevundimonas* catalyzes the incorporation of hydroxyl moieties at the 3, 3' positions on the β-ionone rings and acts on previously ketolated β-ionone ring carotenoids at the 4, 4' positions. The potential products from the actions of CRTZ and W on endogenous carotenoids are illustrated in Fig. 1.

Nicotiana glauca, or the "Tobacco tree", has been used as the host in this study. In part, this is due to its highly pigmented flowers, which have been shown to be responsive to ketocarotenoid

formation (Gerjets et al., 2007). In addition, *N. glauca* has potential as a biorefining raw material feedstock for bioethanol production (National Non-Food Crops Centre, 2011) and valuable hydrocarbon-based fuel components are secreted from the leaf (Mortimer et al., 2012). Its growth characteristics permit cultivation on semi-arid marginal land, yielding large quantities of above ground biomass (Curt and Fernández, 1990) and are nicotine-free. Although the related compound anabasine is present which has been used as an insecticide. Therefore, our aim was to extend the utility of *N. glauca* as a potential biorefinery feedstock possessing added value products, through optimised pathway engineering and utilize the transgenic lines to further our understanding of cellular adaption to the formation of non-endogenous products.

RESULTS

Transformants Expressing *crtZ* and *W* have Diverse Tissue Phenotypes, but all Contain Ketocarotenoids

Following selection of transformants on kanamycin, PCR positive *N. glauca* plants (40 in total), containing both *crt*Z and W, were regenerated. Based on vigor and color, ten plants were cultivated in the glasshouse to maturity and concurrently five non-transgenic (PCR negative) plants were regenerated as controls. These primary (T_0) transformants had no visible differences in their physiology apart from leaf and flower colour (Fig. 2A-G). For example, all those expressing *CrtZ* and W possessed dark brown/green leaves, compared to the green foliage of their wild type counterparts. Line GE15C2S2(1) had the most intense phenotype, with the leaves displaying a red coloration at the extremities (Fig. 2F). Colorimeter readings confirmed these visual changes, with ΔE^*ab values having 10 to 40% increases, compared to the control lines. The most dramatic colour change was observed in the flowers, where an intense red pigmentation was observed compared to the yellow of the controls (Fig. 2G). The chlorophyll and carotenoid contents varied among the T_0 transformants, with chlorophyll significantly lower in 60% of the transformants, higher in 10% and the Chl_a:Chl_b ratio altered in 50%. Total carotenoids showed a similar trend, with 70% having a content lower than the wild type, and 10% with higher levels. Despite these variations, the ratio of chlorophyll: carotenoid was consistent at ca.1:1 (Supplemental Table S1).

In order to quantify and characterize the products from transgenesis, modifications to previously described HPLC systems (Fraser et al., 2000) enabled separation of all mono and bi ketolated, and hydroxylated carotenoids feasible from the action of CRTZ and W. The chromatographic and spectral properties of the endogenous and newly formed carotenoids are provided in Supplemental Table S2. Ten pigments: *cis*-violaxanthin I, *cis*-violaxanthin II, antheraxanthin, chlorophyll a and b, lutein, zeaxanthin, pheophytin, β-carotene and its geometric isomer were identified from an extract of wild type *N. glauca* leaf (Fig. 3A), whilst the presence of CRTZ and W produced novel carotenoids: 4-ketolutein, astaxanthin, 4-ketozeaxanthin, phenicoxanthin, canthaxanthin, 3-hydroxyechinenone and echinenone (Fig. 3B).

The presence of non-endogenous carotenoids in the transgenic *N. glauca* extracts was evident by thin layer chromatography (TLC), compared to wild type counterparts. On the basis of co-chromatography with authentic standards and color, the wild type pigments identified on TLC were chlorophyll, lutein, chlorophyll derivative and β-carotene (Supplemental Fig. S1). The ketocarotenoid contents of the transgenic lines varied. For example, in addition to those carotenoids found in the wild type, lines GE14C2S3 (1), (2), (3) and (6) contained phoenicoxanthin, canthaxanthin, 3- hydroxyechinenone and echinenone, whilst lines (4), (5), (7) and (8) also

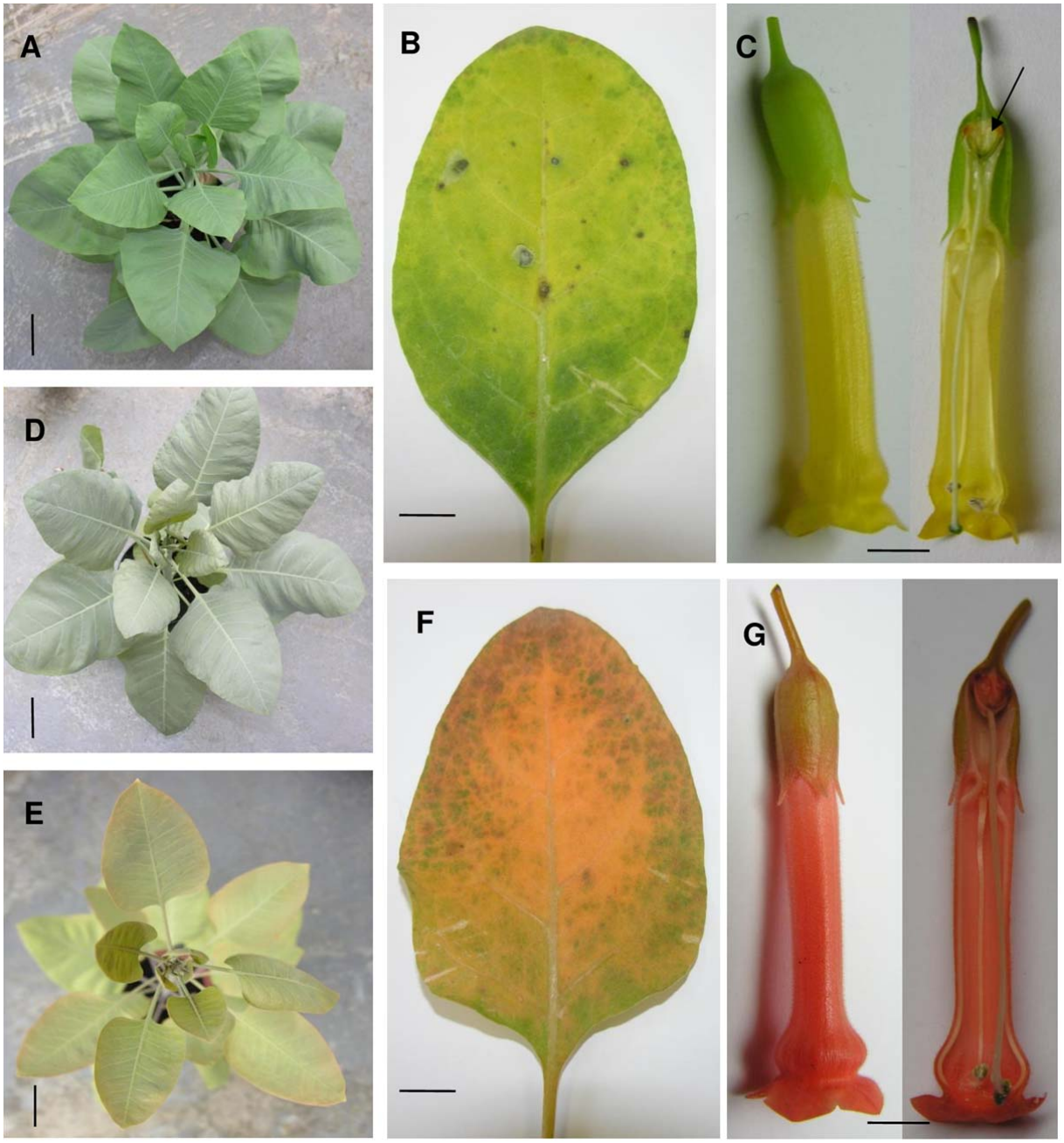

Figure 2. Colour changes in the flowers and aerial parts of transgenic To *N. glauca plants expressing Brevundimonas sp. crtW and crtZ.*

(A) Wild type (WT). (B) Senesced WT leaf. (C) WT flower; ovary and nectary tissue are indicated by upper and lower arrows, respectively. (D-E) Transgenic plants G1 and G7, respectively. (F) Senesced leaf from transgenic plant G1. (G) Transgenic flower. Aerial phenotype in (D) is representative of all recombinant *N. glauca* plants, with the exception of line G7, shown in (E). Floral phenotype in (G) is representative of all recombinant *N. glauca* plants. Bars = 4 cm for (A) (D) and (E), 1cm for (B) (F), and 0.5 cm for (C) and (G).

contained astaxanthin. In line GE29C4S5(9), the only ketocarotenoid found was 3-hydroxyechinenone (Supplemental Table S2). Extracts from flower tissues showed a greater number of intensely colored components on TLC. Astaxanthin, phoenicoxanthin, canthaxanthin, 4-ketozeaxanthin and 3-hydroxyechinenone were present. However, the chromatograms had more

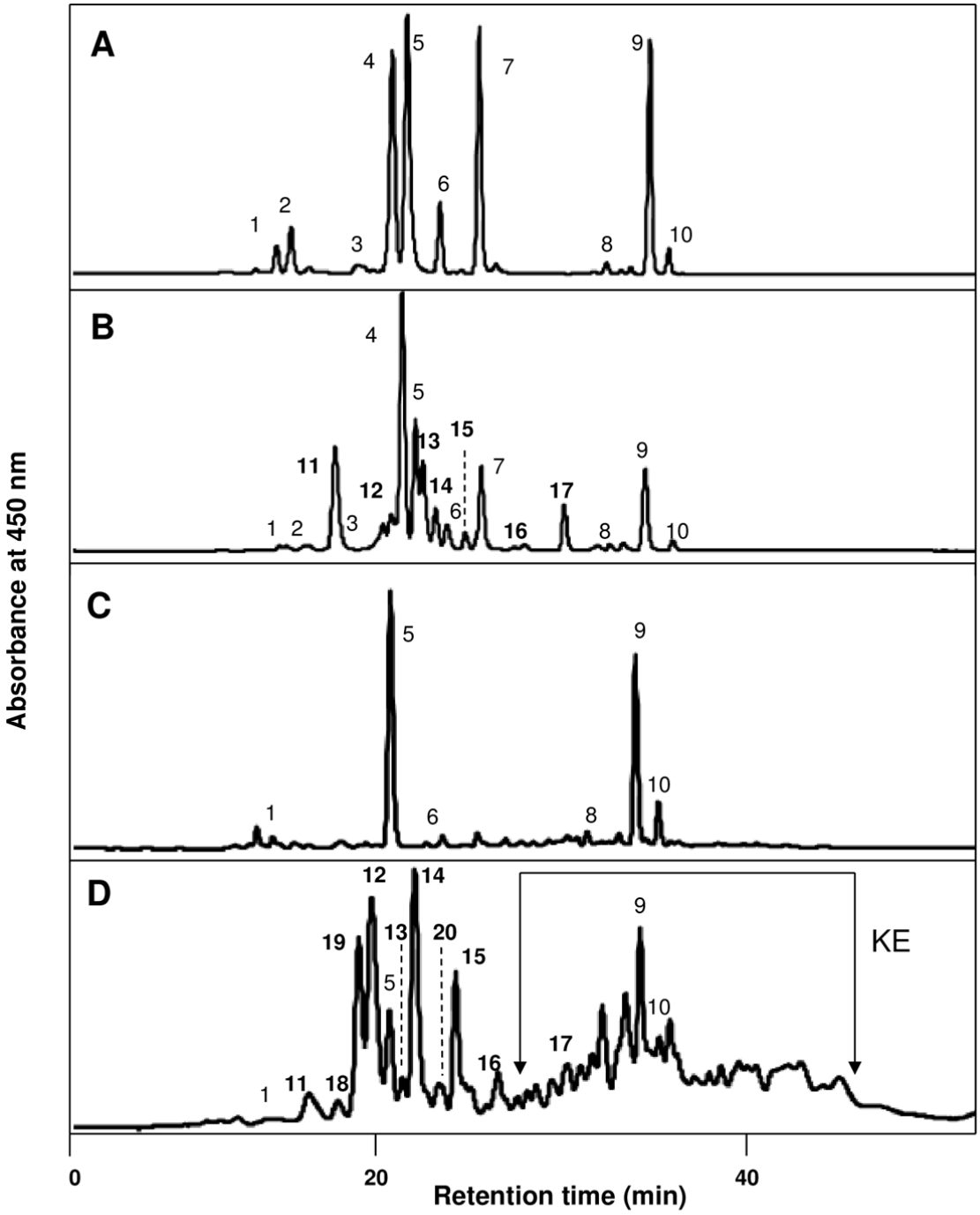

Figure 3. HPLC-Photo diode array (PDA) profiles of carotenoids present in leaf and petal tissue from WT and *crtZ/crtW* transgenic *N. glauca* plants.
(A) WT leaf. (B) *crtZ/crtW* transgenic leaf. (C) WT petal. (D) *crtZ/crtW t*ransgenic petal. Each component is labelled. Those labelled 11-20 (in bold) and KE (ketocarotenoid esters) were unique to transgenic plants. Component 19 in (B) was identified as a novel ketocarotenoid. See Supplemental Table S2 for spectral and chromatographic properties.

187 diffuse banding in the Rf region from 0.5 to 0.8 (Supplemental Fig. S1). These components co-

188 chromatographed with authentic ketocarotenoids esters derived from *Haematococcus* cysts or

189 *Adonis* flowers. Thus, esterified keto/hydroxylated carotenoids were present, as was a band with a
190 Rf of 0.1, below astaxanthin, in the flower tissues (Supplemental Fig. S1).
191 The amounts of individual carotenoids within T_0 lines are provided in Supplemental Table
192 S1. The proportion of ketocarotenoids in leaf material varied in the T_0 population from 2% to 55%
193 of the total carotenoids. For example, line GE14C2S3(1) contained total carotenoids of 5.14 ±
194 0.32 μg/ mg, compared to 6.44 ± 0.2 found in the wild type. The total ketocarotenoid content was
195 40% of the total, with 20% 4-ketolutein, 7% ketozeaxanthin and 2% astaxanthin. During leaf
196 development and senescence a phenotypic difference between the wild type and the *crtZ*/*W* lines
197 was observed, with the latter becoming more red/pink in color. As expected, there was a dramatic
198 loss of chlorophyll in senescing leaves and a reduced content of endogenous and non-endogenous
199 carotenoids, but not of phytoene and ketocarotenoid esters. Interestingly, the proportion of
200 ketocarotenoids present did not alter in young or mature stages nor senescing material. No
201 esterification of ketocarotenoids in the expanding and mature leaves occurred, but in senescing
202 material 50% of the ketocarotenoids were esterified (Table 2).
203 The greatest changes in carotenoid content were found in transgenic *N. glauca* flower tissues.
204 In wild type flowers lutein, zeaxanthin, β-carotene, and its isomer were present (Figure 3 C). These
205 carotenoids decreased when CRTZ and W were present (Fig. 3D), resulting in the appearance of 4-
206 ketolutein, astaxanthin, 4-ketozeaxanthin, phoenicoxanthin, 3'-hydroxyechinenone, canthaxanthin
207 and echinenone. Co-chromatography with ketocarotenoid esters from *Haematococcus* cysts and the
208 *Adonis* flower material, showed that a number ketocarotenoid esters where formed (Fig. 3D). These
209 esters displayed "bell"-shaped spectra, typical of ketocarotenoids, with spectral maxima between
210 465 and 477 nm. Therefore, we presume that these esterified ketocarotenoid species were a mixture
211 of astaxanthin and 4-ketozeaxanthin esters. Based on the comparative chromatographic properties
212 of authentic, diesterified forms of astaxanthin; it is likely that the formation of diesters
213 predominates in the *CrtZ*/*W N. glauca* flowers. A more polar carotenoid than astaxanthin, with a
214 monoketolated-like UV/Vis spectra, and a maximum at 470nm, was also detected (Fig. 3D, peak
215 19). On reduction with $NaBH_4$, a β-carotene-like spectrum, with a 450nm maximum, was found.
216 HPLC fractionation, followed by high resolution MS analysis, gave rise to a compound with a
217 581.399 Da [M+H]+ ion, corresponding to a monoisotopic mass of 580.392 Da. These masses infer
218 a molecular formula of C_{40} $H_{52}O_3$ having a mass of 580.839. A putative carotenoid having this mass
219 could be 3-hydroxyechinenone epoxide. Further support for this compound came from MS
220 components resulting from in-source fragmentation. The ions included 563.389 Da ($C_{40}H_{61}O_2$)
221 suggesting the loss of a hydroxyl moiety (-17.003 Da), as water; 564.397Da was detected inferring
222 $C_{40}H_{52}O_2$ which could arise from the loss of an epoxide and ring rearrangement and 547.394 Da
223 (C_{40} H_{61} O) was also found which could have resulted from the loss of OH as water, after

fragmentation of the epoxide group and ring rearrangement. The presence of a monoepoxide was further revealed by TLC separation of the enriched fraction and staining in the presence of trifluoroacetic acid vapor, to yield a color change from deep orange/red to green.

In transgenic petals, there was a 2 to 3 fold increase in total carotenoids. The ketocarotenoid content of the petals represented 78 to 82% of the total carotenoids. Esterified ketocarotenoids were the most abundant, representing 51 to 61% of the total, with astaxanthin mono- and di-esters being the most common. The individual endogenous carotenoids present in the petal tissue were phytoene, lutein, β-carotene, zeaxanthin, and violaxanthin, of which lutein predominated. In the transgenic lines several newly formed ketocarotenoids were determined (Table1). Astaxanthin and 3-hydroxy-epoxyechinenone were the most abundant ketocarotenoids amongst those not esterified. The ovary and nectary tissue contained a quantitatively different profile of endogenous carotenoids, with β-carotene predominating, rather than lutein, as found in the petal tissue. The ketocarotenoids found in the petal tissue were also found in the ovary and nectary. However, the proportions were different, with canthaxanthin and phoenicoxanthin being the most abundant free ketocarotenoids (7 and 6%, respectively). Astaxanthin was mainly in an esterified form. The total ketocarotenoid content, including the esters represented 80 to 85% of the total carotenoids, which itself was increased 4 to 6.3 fold in the ovary and nectary tissue, of transgenic lines. Interestingly, despite being the direct precursor, the β-carotene content was not reduced significantly and phytoene increased (up to 20 fold). Lutein, zeaxanthin and violaxanthin levels were reduced by 4, 50 and 3 fold, respectively.

The carotenoid phenotype is inherited in homozygous lines expressing *crtZ* and *W*

Seeds from T_0 lines GE14C2S3(1), GE15C2S2(7) and GE5C4S5(8) (subsequently referred to as lines G1, G7 and G8, respectively), which displayed vigour and the highest ketocarotenoid contents, were germinated and subjected to segregation analysis against kanamycin sensitivity and the presence of the *npt*II gene to determine insert number. Mendelian inheritance was found in lines G1 and G7, i.e., azygous 20-25%, hemizygous 45-55% and homozygous 25-35%. The presence of the *npt*II was also confirmed. In contrast, the kanamycin sensitivity of the G8 seedlings was not consistent with Mendelian inheritance. Ten *npt*II homozygous and hemizygous plants from G1-T_1 and G7-T_1 and ten plants from the G8 lines were cultivated. The T_1 generation of the homozygous lines of G1 and G7 showed mixed phenotypes to the To generation. For example, homozygous lines from the G1 T_1 plants had three phenotypes, (i) - 6 plants had the characteristic dark brown/green leaves of the T_0 generation and red pigmented flowers, (ii)- 2 plants had leaves with dark brown and green patches and uneven pigmentation of the flowers, while (iii) 2 plants had yellow colored flowers and were indistinguishable from the wild type. No notable differences in

growth rate or size were observed. qRT-PCR, using the endogenous *Pds* gene as the single copy calibrator, confirmed the zygosity assigned from the sensitivity to kanamycin and *npt*II presence. Thus, a percentage of G1-T_1 lines displayed the wild type phenotype, but molecular analysis indicated they were homozygous.

CrtZ and *W* transcript levels showed an 80% reduction in phenotype 2, compared to phenotype 1. Those lines displaying phenotype 3 expressed *crtZ* and *W* transcripts at very low (1-2%) levels, suggesting that transcriptional gene silencing had occurred. In all cases, the novel carotenoids in the T_1 lines were 4-ketolutein, echinenone, 3-hydroxyechinenone, canthaxanthin, phoenicoxanthin, 4-ketozeaxanthin and astaxanthin, with the predominant ketocarotenoids being 4-ketolutein (5 to 20% of the total carotenoid) and 4-ketozeaxanthin (3 to 9% of the total carotenoid). Among the endogenous carotenoids, β-carotene, lutein, antheraxanthin and violaxanthin were reduced in all T_1 plants with the dark brown phenotype; violaxanthin and lutein contents being reduced most significantly. Zeaxanthin increased in all T_1 lines, and phytoene appeared in all *crtZ* and *W* T_1 lines. The pigment content of the T_1 flower tissues was similar to that obtained in the T_0 generation, with the exception of silenced lines (Table 1).

Sequestration of non-endogenous carotenoids

The mechanisms associated with the storage of these compounds were investigated in the T_1 lines. Isolated chloroplasts were separated into stroma, plastid membranes and plastoglobules enriched fractions. The purity and identity of the fractions were confirmed by the immunodetection of known proteins with well characterised plastidial locations. Plastoglobulin 35 (PGL35) was used to indicate plastoglobule enrichment, the thylakoid-associated D1 protein of PSII (PsbA) to identify plastid membranes and RuBisCO (Rbcl) the stromal marker. In all cases, immunodetection of the protein marker for a particular fraction occurred, with only minor cross-reactivity among fractions (Fig. 4).

No carotenoids where found in the stromal fraction of the wild type, or transgenic lines. Although the plastoglobules contained only a small proportion (0.03%) of the carotenoids found in the plastid. G1 and G7 contained a 5 and 25-fold increase, respectively, in the carotenoid content of the plastoglobule compared to the wild type. The endogenous carotenoids found in the plastoglobule fraction were phytoene, β-carotene, lutein and violaxanthin. In the transgenic genotypes, these endogenous carotenoids increased dramatically in the plastoglobules. For example, a 50 to 100 fold elevation in phytoene was detected; representing nearly 50% of the plastoglobule carotenoid content in the transgenic lines. Violaxanthin did not change significantly, but zeaxanthin and antheraxanthin were detected uniquely in the transgenic lines. Of the ketocarotenoids, 4-

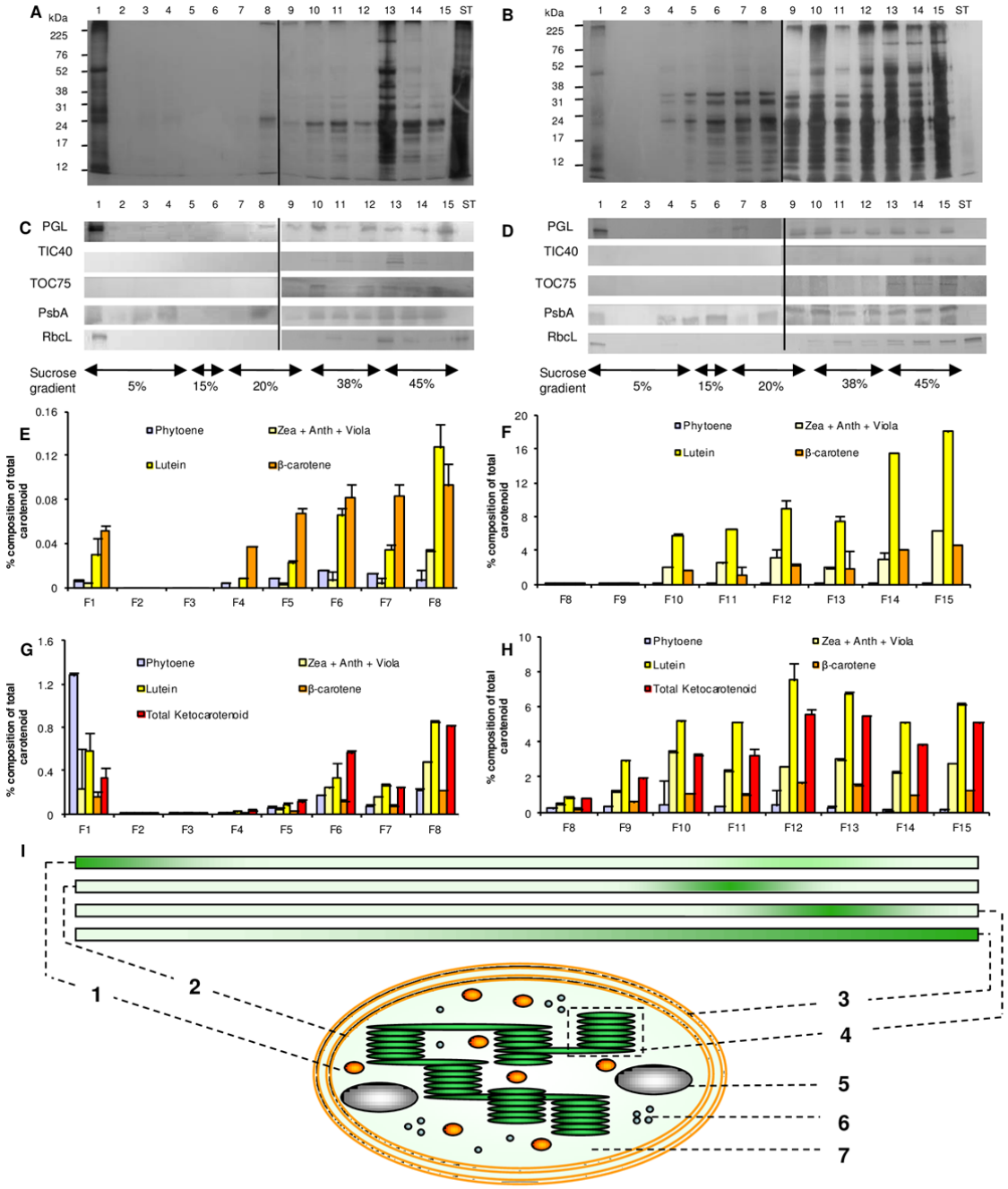

Figure 4. SDS-PAGE separation and immunoblot analysis of WT and *crtZ/crtW* transgenic, chloroplast fractions.
(A-B) SDS-Page separation of WT (A) and G1 (B) chloroplast fractions. Total membranes from isolated chloroplasts were separated by flotation on a discontinuous sucrose gradient. Gradients were prepared from three separate plastid preparations. Fractions from the 3 separate gradients were pooled. Fractions 1 to 15 in addition to stromal preparations (ST) are indicated. (C-D) Immunoblot analysis of WT (C) and G1 (D) chloroplast fractions. Immunoblot analysis was performed using marker antibodies (Agrisera). PVDF membranes were probed successively with antisera raised against plastoglobulin 35 (PGL35, 35kDa); chloroplast inner envelope membrane translocon complex protein (TIC40, 40kDa); chloroplast outer envelope membrane translocon complex protein (TOC75, 75kDa): thylakoid-associated D1 protein of PSII, (PsbA, 38kDa) and the stromal large subunit of RuBisCO (RbcL, 52kDa). (E-H) HPLC-PDA analysis of WT (E, F) and G1 (G, H) chloroplast fractions.Viola, violaxanthin; Neo, Neoxanthin; Zea, Zeaxanthin. Values are the average of three replicates, from pooled fractions of three independent discontinues sucrose gradients. Error bars indicate +SEM. (I) Schematic representation of the abundance of chloroplast ultrastructures throughout sucrose gradients. An increase in colour intensity in each bar represents an increase in the abundance of the indicated structure, respective to the fractions in the panels above (E and H). (1) plastoglobules; (2) inner chloroplast envelope; (3) outer chloroplast envelope; (4) thylakoid membrane (grana); (5) starch granule; (6) ribosome; (7) stroma..

294 ketolutein was the most predominant. In total, the ketocarotenoids represented 10 to 20% of the
295 total carotenoid content of the plastoglobule (Table 1).

Unlike the plastoglobule, total carotenoids in the plastid membrane fraction displayed relatively minor fluctuations in content among the transgenic genotypes and their wild type comparator. However, phytoene accumulated to 6% of the total carotenoid content. Zeaxanthin levels increased significantly in the transgenic genotypes, whilst lutein and violaxanthin were reduced. β-Carotene and antheraxanthin levels did not change dramatically in the plastid membranes. The range and abundance of ketocarotenoids (astaxanthin, 4-ketozeaxanthin, phenicoxanthin, canthaxanthin, 3-hydroxy echinenone, echinenone and 4-ketolutein) in the membrane were similar to the plastoglobule, with the exception that 4-ketozeaxanthin was detected. The proportion of total ketocarotenoids in the plastid membranes of G1 or G7 was 25 and 18% of the total pigment, respectively. Quantitatively the membrane remained the main site of carotenoid sequestration.

In order to analyse the different plastid membranes further, chloroplasts were isolated, broken by osmotic shock and sub-fractionated.. An immunodetection approach was then used to probe the different fractions for known proteins with well characterised sub-plastidial locations. Although complete separation between the marker proteins and thus the sub-plastid organelle components was not possible, enrichments across fractions was achieved. For example plastoglobulin 35 (PGL35) was detected in fraction (F)1 predominantly, but also F2 to 4 and then again in F8 to 15 (Figs. 4 A and B). The chloroplast inner envelope membrane translocon complex protein (TIC40) was predominantly found in F10 to 14, while the chloroplast outer envelope membrane translocon complex protein (TOC75) was more pronounced in F13 to 15. The thylakoid-associated D1 protein of PSII (PsbA) was strongly detected in F10 to 15. RuBisCO (Rbcl), a stromal marker, was found in F12 to 15. In all cases the immuno-reactive bands corresponded to the predicted MW of the target proteins. Comparison between the wild type and transgenic lines used showed a consistent profile. From these data it was predicted that the plastoglobule component predominated in F1, but the presence of PGL 35 in F8 to 15 suggested the protein, and perhaps the plastoglobules, are derived from the thylakoid membrane. Thylakoid membrane components (as indicated by the PsbA protein) were present in F10 to F15 but displayed the greatest enrichment in F12 to 14. Interspersed within the presence of the thylakoid material was the enrichment of the inner envelope membrane F10 to 14 and outer envelope membrane F13 to 15. Stroma, probably derived from thylakoid lumen, was also detected in F12 to 15 as indicated by RuBisCO (Fig. 4). The carotenoid content of the wild type plastoglobule fractions represented 0.05% of the total carotenoid found across the gradient (membrane fractions). In the transgenic lines this proportion increased 30-fold. Wild type-derived plastoglobules contained β-carotene as the predominant carotenoid, with phytoene detectable. In contrast, the transgenic plastoglobules contained phytoene as the abundant carotenoid and β-carotene the least abundant. Several ketocarotenoids, including

astaxanthin, 4-ketozeaxanthin, phenicoxanthin, canthaxanthin, 3-hydroxy echinenone, echinenone and 4-ketolutein were also found; collectively the ketocarotenoids represented 25% of the carotenoids found in the plastoglobule. These data corroborated the isolation procedure described earlier. Lutein, zeaxanthin, antheraxanthin, violaxanthin and β-carotene and trace levels of phytoene were found throughout wild type fractions 8 to 15. However, the average ratio of zeaxanthin, antheraxanthin and violaxanthin (ZAV):lutein:β-carotene was 1:3:1 in F10 to F13, with lutein representing 60%, ZAV 20% and β-carotene 20% of the total pigment in the fractions. In F14 and 15 the ratio of ZAV:lutein:β-carotene was 1:5:1 with lutein being 70%, ZAV 14% and β-carotene 10% of the total carotenoid per fraction. Collectively, fractions derived from the transgenic genotypes showed no significant changes in the amount of carotenoid per membrane fraction. From F10 to 15 there was a consistent ratio averaging 1:2.2:0.4:1.6 between ZAV:lutein: β-carotene: ketocarotenoid. In the absence of ketocarotenoids the proportions of the total carotenoid content per fraction for ZAV, lutein and β-carotene were 27, 61 and 10%, respectively. On a quantitative basis, lutein levels were reduced to nearly 50%.

Carotenoids in Photosynthetic Complexes Differ in the *crtZ*/*W* Transgenic Plants compared to the Wild Type

The photosynthetic pigment complexes were analyzed to ascertain the incorporation of ketocarotenoids. From the wild type and 2 transgenic lines ((G1 and G7 the core complex I (CCI), core complex II (LHCII monomer) and trimeric light harvesting complex II (LHCII trimer) were separated and identified as described in Dörmann et al (1995) and Lokstein et al (2002) and by GEL-LC-MS/MS proteomic analysis (Supplemental Table S3). In both transgenic lines the amount,

as judged by intensity, of LHCII trimer was significantly reduced by 50% ($p<0.05$), while the LHCII monomer increased significantly (about 50%; Fig. 5A). Echinenone and 4-ketolutein were found in all the photosynthetic complexes. Comparison of the wild type and transgenic CC1 pigment composition indicted that the proportion of β-carotene remained constant, but that lutein was replaced by echinenone in the transgenic varieties (Table 3). The LHCII trimer contained a

359 consistent (80%) level of lutein, but 4-ketolutein replaced zeaxanthin and violaxanthin in both the
360 transgenic varieties. The CCII and LHC monomer mirrored their CCI and LHCII trimer
361 counterparts (Fig. 5B). In comparison to the wild type, both G1 and G7 had significantly reduced
362 ($p<0.05$) Fv/Fm values. In the latter, the Fv/Fm value was reduced to almost 50% of that of the wild
363 type. This line displayed the greatest change in the carotenoid composition of pigment-protein

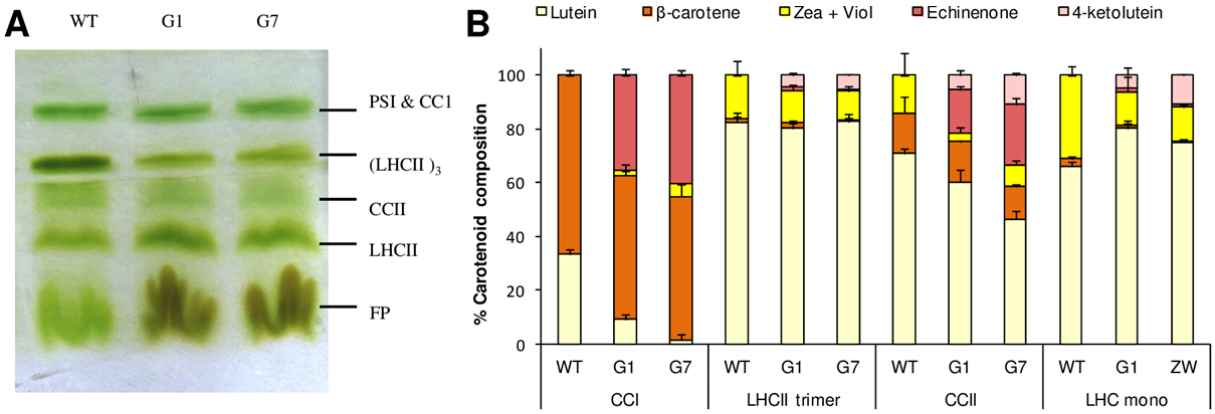

Figure 5. Distribution of carotenoids within photosynthetic complexes isolated from WT and *crtW/crtZ* transgenic *N. glauca* plastids. .

(A) Partially denaturing 'green' gel, electrophoretic separation, of pigment-protein complexes from WT and transgenic plastid preparations. (B) Pigment composition of isolated photosynthetic complexes. % compositions were calculated from total carotenoids extracted for each gel band and are the average of three values from complexes isolated from separate plastid preparations. Error bars indicate +SEM. CCI, core complex 1; CCII core complex II, LHCII monomer, monomeric form of light harvesting complex II; LHCII trimer, trimeric form of light harvesting complex II; LHCI light harvesting complex I.

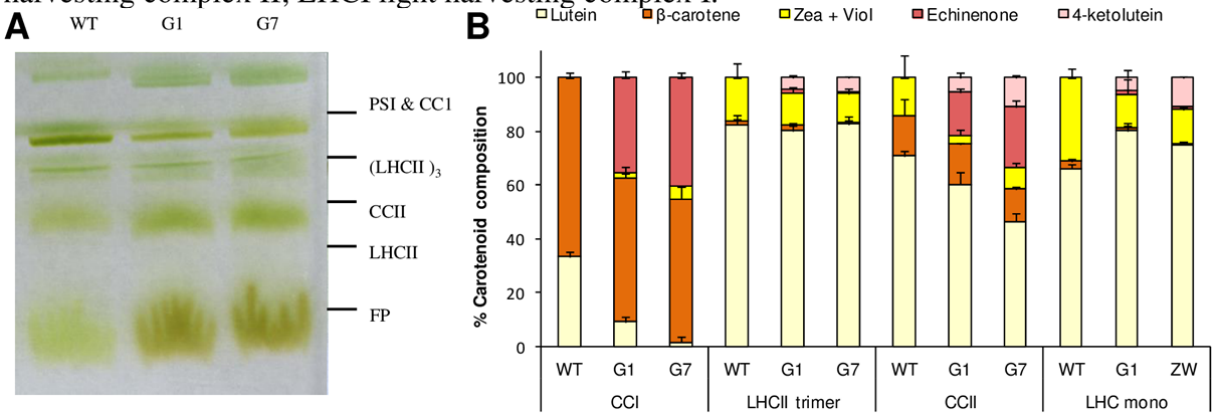

Figure 5. Distribution of carotenoids within photosynthetic complexes isolated from WT and *crtW/crtZ* transgenic *N. glauca* plastids. .

(A) Partially denaturing 'green' gel, electrophoretic separation, of pigment-protein complexes from WT and transgenic plastid preparations. (B) Pigment composition of isolated photosynthetic complexes. % compositions were calculated from total carotenoids extracted for each gel band and are the average of three values from complexes isolated from separate plastid preparations. Error bars indicate +SEM. CCI, core complex 1; CCII core complex II, LHCII monomer, monomeric form of light harvesting complex II; LHCII trimer, trimeric form of light harvesting complex II; LHCI light harvesting complex I.

364 complexes, a reduced chlorophyll content (16% of the wild type), although the ratio of chlorophyll

365 a/b was not altered (Supplemental Table S4).

366

367 **Cells of Transgenic Lines show Changes in Ultrastructure and Metabolite Pools**

To determine the effects of the ketocarotenoids at the cellular level, transmission electron microscopy (TEM) was carried out, whilst perturbations in metabolism were analyzed by metabolite profiling.

(i) The plastid ultrastructure changed in transgenic lines

Although light microscopy showed no observable alterations to the leaf and flower cells, TEM revealed significant ultrastructural changes to the plastids. In comparison to the wild type, chloroplasts of the *crtZ*/*W* genotypes were reduced (approx. 2-fold) in area, but the number of chloroplasts per cell remained the same. There was a virtual absence (< 5%) of starch granules within the plastids derived from the transgenic lines (Fig. 6A-D). A comparison between plastid areas, minus the area occupied by the starch granules, indicated that the chloroplast area of the wild type and transgenics was comparable. More plastoglobules per plastid were observed in the transgenic lines, but were reduced in area. Collectively, the total plastoglobule area per plastid was similar (wild type 0.24μm^2 and transgenic 0.21μm^2). The morphology of the transgenic plastoglobules was clearly different, with much more intense staining, presumably reflecting a different composition (Fig. 8). No significant difference between the wild type and transgenic lines was found in the thylakoid area per plastid, or number of grana per plastid. In both cases, the chromoplasts in the flower tissues had a similar ultrastructure, with plastoglobules dominating the chromoplasts (Fig. 7A-D). However, the plastoglobules of transgenic floral tissue were much larger in area in comparison to the wild type.

(ii) Ketocarotenoid Formation Caused Changes to Metabolite Composition of Leaf and Petal

Individual metabolites were analysed for significant perturbations using student's *t*-tests (Table 4). Analyses were carried out on leaf from two independent events, both genotypes displayed similar changes in their metabolome. For example in the leaf the levels of amino acids showed the greatest reductions, particularly those derived from pyruvate and localized in the plastid. Phytosterol content was also significantly increased in the leaf material derived from these genotypes. In contrast, the flower petal exhibited increased amino acid content in comparison to the wild type.

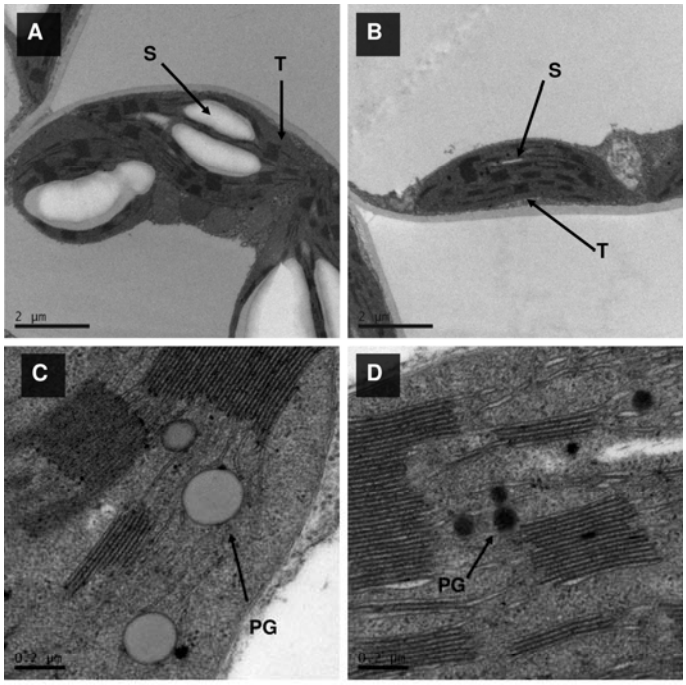

Figure 6. Changes in leaf plastid ultrastructure resulting from the expression of *Brevundimonas* sp. *crtW* and *crtZ*.
(A) WT plastid. (B) G1 plastid. (C) WT plastoglobules. (D) G1 plastoglobules. S, starch granule; T, thylakoid membrane; PG, plastoglobule. Scale bars are indicated in each panel. Sections were prepared from transverse sections of three leaves, representative sections have been illustrated.

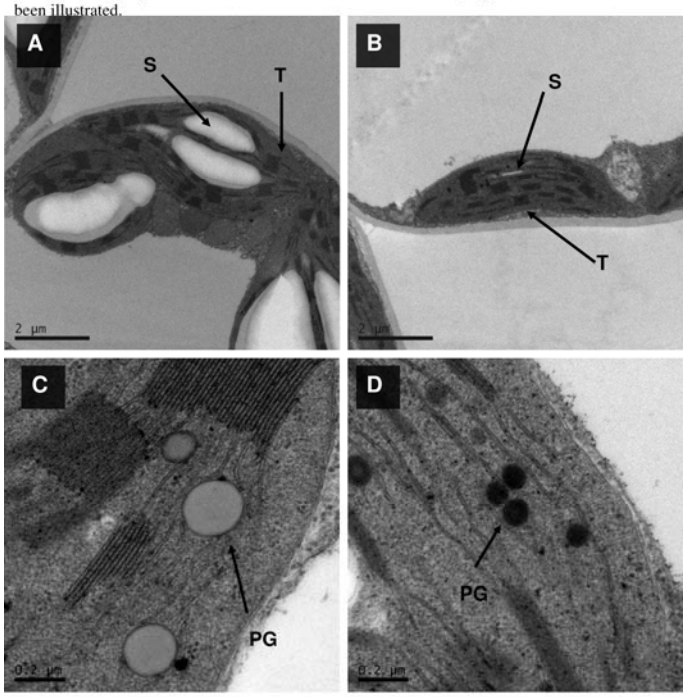

Figure 6. Changes in leaf plastid ultrastructure resulting from the expression of *Brevundimonas* sp. *crtW* and *crtZ*.
(A) WT plastid. (B) G1 plastid. (C) WT plastoglobules. (D) G1 plastoglobules. S, starch granule; T, thylakoid membrane; PG, plastoglobule. Scale bars are indicated in each panel. Sections were prepared from transverse sections of three leaves, representative sections have been illustrated.

399 **DISCUSSION**

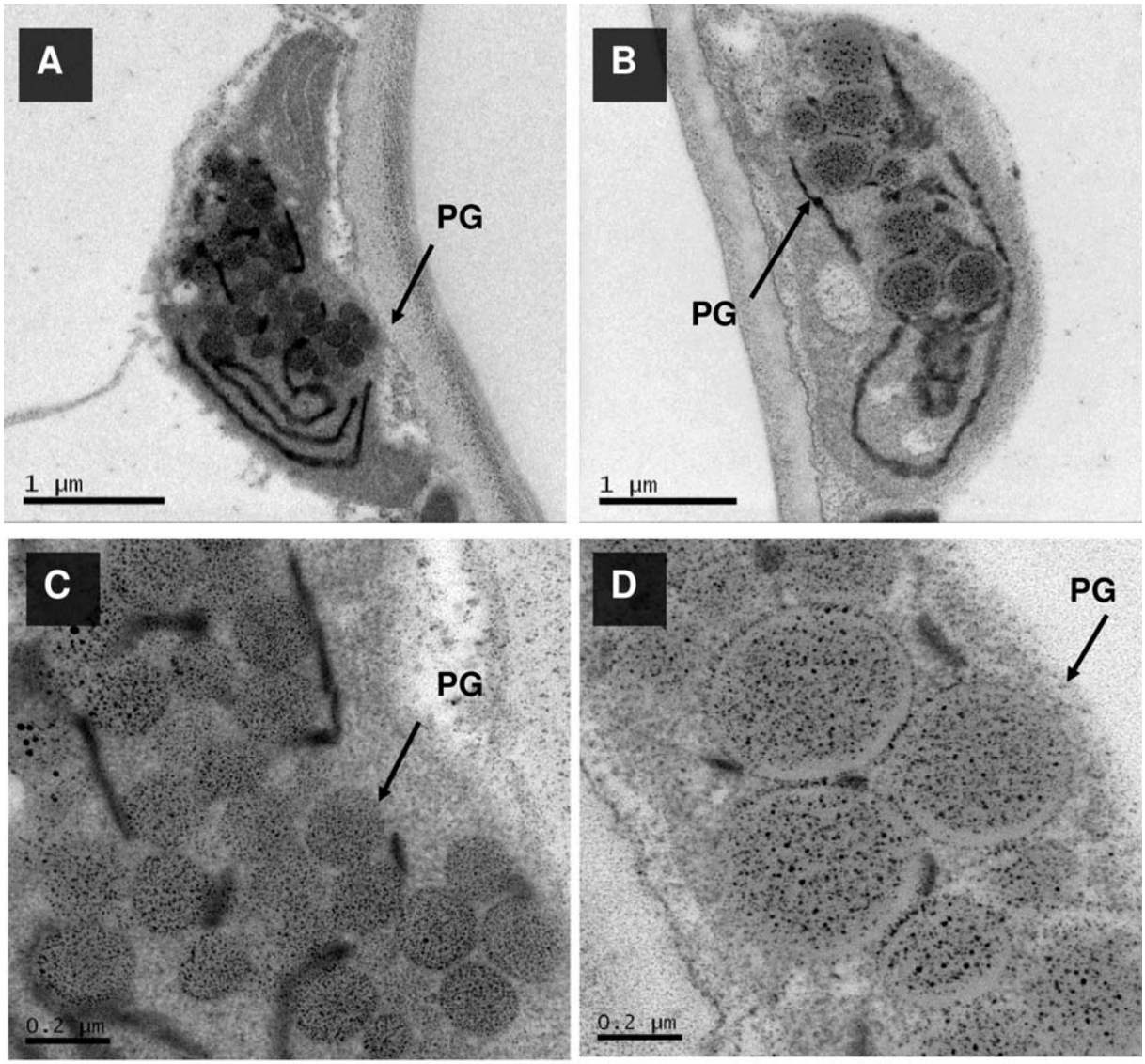

Figure 7. Changes in petal plastid ultrastructure resulting from the expression of *Brevundimonas* sp. *crtW* and *crtZ*.
(A) WT plastid. (B) G1) plastid. (C) WT plastoglobules. (D) G1 plastoglobules. PG, plastoglobule. Scale bars are indicated in each panel. Sections were prepared from transverse sections of three flowers; representative sections have been illustrated.

The transgenic genotypes of *N. glauca* expressing the *crtZ* and *W* contained ketocarotenoids that are not present in the wild type vegetative tissues. In addition, an increase in hydroxylated carotenoids, such as zeaxanthin, was observed (Table 1). Thus, both the *Brevundimonas* CRTZ and W enzymes are functional and act to modify the endogenous carotenoids. The array of compounds formed, however, suggests that they are not under coordinated regulation, but act in a random, promiscuous manner upon the surrogate precursors being available. For example, 4-ketolutein is formed by the action of the oxygenase on the endogenous lutein in photosynthetic tissues. The formation of a mono-ketolated product correlates with *in vitro* enzyme data (Fraser et al., 1998), showing activity solely with β-ionone rings.

409 The collective data of the transgenic genotypes in the T_2 generation, suggest no dramatic increase in
410 the total carotenoid content, although the accumulation of phytoene in the transgenic lines and
411 reduced β-carotene suggests an increase in early pathway flux to deliver precursors of the
412 ketocarotenoids. Although it cannot be ruled out that the desaturation of phytoene is acting as a
413 restriction in the pathway, resulting in phytoene accumulation. Between the α-and β-ring-derived
414 branches of the carotenoid pathway, the latter is disrupted most significantly, with reduced
415 formation of violaxanthin and zeaxanthin due to the conversion into 4-ketozeaxanthin and
416 astaxanthin. This routing of precursors may be a result of the bacterial hydroxylase acting in a more
417 complementary manner with the *crtW* gene products, in comparison to the plant derived
418 hydroxylases, as both of the latter (*Cyp97 A* and *C*) are upregulated in transgenic leaf (Supplemental
419 Table S5). The formation of echinenone, canthaxanthin, phoenicoxanthin and astaxanthin shows
420 that the transgene products and/or the plant hydroxylases have combined to create this biosynthetic
421 route to astaxanthin. In the case of the ε-carotene pathway, only the end-products have been
422 modified, suggesting stricter metabolic regulation of the α- pathway, compared to its β- counterpart.
423 In transgenic flower tissues, the levels of ketocarotenoids were higher than in photosynthetic tissues
424 (Table 1) and also qualitatively different. The expression of endogenous genes was also unlike that
425 in vegetative cells (Table 4). Those genes encoding enzymes for the ε– pathway were down-
426 regulated in transgenic tissues, presumably maximizing flux into the β –pathway and the subsequent
427 ketocarotenoids. These changes in the enhancement of β-ring carotenoids are also reflected by the
428 presence of the carotenoid putatively designated as 3-hydroxyechinenone. This rare/new carotenoid
429 requires further testing and NMR analysis in order to unambiguously assign chemical structure. The
430 only previous report of *N.glauca* modified with a cyanobacterial derived ketolase, showed increased
431 β-ring derived carotenoids, but in comparison the levels where lower and due to the enzyme
432 specificity the end-product was the mon-ketolated product, 4-ketozeaxanthin (Gerjets et al. 2007).
433 The disassembly of thylakoid membranes and photosynthetic complexes, appearance of
434 plastoglobules and degradation of pigments during senescence have been documented (Brehelin et
435 al., 2007; Thomas et al., 2009). The endogenous and to a lesser extent non-endogenous pigments
436 support this phenomenon. It is feasible that membrane disruption could affect the electron transport
437 chain necessary for efficient desaturation both in green and non-green tissue (Josse et al., 2000).
438 This could then contribute to the accumulation of phytoene through the impaired desaturation
439 and/or isomerization. For example, altered plastoquinone levels have a detrimental effect on the
440 carotene desaturation sequence resulting in increased phytoene (Norris et al., 1995).
441 The mechanisms by which carotenoids are degraded could involve enzymatic catabolism involving
442 carotenoid cleavage dioxygenases (CCDs), (Auldridge et al 2006; Bruno et al., 2016) and non-

443 enzymatic approaches associated with lipid peroxidation and reactive oxygen species (ROS)
444 quenching (Dambeck and Sandmann, 2014). Recently, reports have illustrated the rapidity and
445 importance of carotenoid homeostasis (Latari et al., 2015). It is therefore feasible that the
446 ketocarotenoids are being metabolised in a similar manner to those proposed for the endogenous
447 carotenoids present. In the case of ketolated/hydroxycarotenoids, modification by fatty acid
448 esterification appears to delay the degradation. This may reflect the promiscuous activities of acyl
449 transferases for hydroxycarotenoids that have undergone prior ketolation. Such an observation does
450 have analogy with the phytol ester synthase (PES) enzymes which esterifies toxic phytol (Lippold et
451 al 2012), that is liberated upon chlorophyll degradation a process synonymous with senescence.
452 The demonstration of the formation and accumulation of non-endogenous carotenoids raises in
453 transgenic lines the question of where such pigments are sequestrated. Carotenoid storage
454 lipoproteins have been found in potato (Li et al., 2012), pepper (Simkin et al., 2007) and more
455 recently tomato chromoplasts (Nogueira et al., 2013). In the present study, separation of sub-
456 plastidial components, in conjunction with microscopy, were adopted. The plastid membrane
457 fractions contained the largest variety of carotenoids, but no quantitative differences were observed
458 between the wild type and *crtZ*/*W* transgenic lines. Qualitatively, the level of lutein present in
459 transgenic membranes was reduced and displaced by ketocarotenoids. The unique presence of
460 phytoene in the membrane fractions of the transgenic lines (Table 1) suggests that the pathway had
461 been activated to produce precursors, either in response to increased end-product utilization
462 (forward-feed mechanisms), or the removal of an initiator of negative feedback. It has been
463 postulated that desaturation intermediates in the *cis* geometric state act as substrates for enzymatic
464 cleavage and these molecules (which are yet to be identified) act as retrograde signaling molecules
465 controlling transcriptional regulation of the pathway. This proposition has recently been questioned,
466 due to the inability of carotenoid Cleavage Dioxygenase (CCD)-4 to act on acyclic carotenes
467 (Bruno et al., 2016) and the lack of phenotypic or metabolic changes in transgenic tomato plants
468 that produce the CRTI gene product. In the latter case the CRTI was shown to eliminate the
469 presence of cis-carotenes with no effects on the plants phenotype (Enfissi et al., 2016). The
470 carotenoid profile indicated a reduced composition in lutein compared to zeaxanthin, antheraxanthin,
471 violaxanthin and neoxanthin in those fractions where TIC75 and TOC40 predominated. These
472 findings indicate the presence of envelope and thylakoid at the onset of the membrane fractions,
473 followed by thylakoids in a higher purity as the density of the gradient increases. Ketocarotenoids
474 were present throughout the membrane fractions, with a consistent composition (Fig. 4E-H). Thus,
475 from these data, ketocarotenoids are present both in the envelope and thylakoid membranes.
476 The plastoglobule fraction had the lowest density and was confirmed by the presence of the
477 plastoglobulin (fibrillin) protein. In comparison to the membrane fraction, the amount of

carotenoids present in the plastoglobule was low. However, substantial increases in carotenoid content were apparent in the transgenic lines, compared to the wild type derived plastoglobules (Figure 4). This increase included the presence of ketocarotenoids, but most striking was the elevation of phytoene. It has been well documented that xanthophylls, such as zeaxanthin with polar head groups conferred by hydroxylation of the C3 and C3′ positions on the β-ionone rings, act to stabilize the membrane phospholipid bilayer (Havaux et al., 2007). In contrast, the hydrocarbon phytoene displays mobility within the membrane bilayer. As such, an accumulation of phytoene in the thylakoid or envelope membrane could lead to membrane instability. Therefore, it is likely that additional phytoene within transgenic plastids is sequestrated within the plastoglobule. Interestingly, a second peak of plastoglobules is observed adjacent and converging into the thylakoid fractions (Fig. 4). This corroborates the view that plastoglobules, and therefore the phytoene, originated in the thylakoid (Austin et al., 2006). This finding is similar to the recent chromoplast study, where phytoene was present in the plastoglobule, but in contrast reduced when endogenous pigments were increased (Nogueira et al., 2013). The increase/altered plastoglobule content in *N.glauca* leaves and flowers and tomato fruit in response to changes in carotenoid levels would appear to be different to *Capsicum*, where fibrils prevail (Deruere et al., 1994).

It has been postulated that phytoene synthase is the rate limiting step in carotenoid biosynthesis (Chamovitz et al., 1993; Fraser et al., 1994), but the accumulation of phytoene suggests the proceeding enzyme in the pathway, phytoene desaturase (PDS), has a key regulatory role in determining flux in these plants. In addition, accumulation of phytoene in the membrane, leading to the packaging of the molecule into the plastoglobule, suggests that a sub-cellular regulation operates within carotenoid biosynthesis. It would appear that metabolites can be dynamically partitioned into different sub-organelle components. Whether the accumulated phytoene is metabolically inert, or can be utilized as a substrate for PDS remains to be explored. Analysis of plastid ultrastructure, revealed an increased number of plastoglobules in the transgenic plastids in the leaves of transgenic *crtZ* and *W* lines compared to the wild type (Fig.. 6). However, the plastoglobules were smaller in size and exhibited denser staining, suggesting that the composition of the plastoglobule has been altered in the transgenic lines. This could be a direct consequence of the increased quantity of non-endogenous carotenoids present or effects on the other lipids associated with plastoglobule. It is possible that the reduced plastoglobule size results from the disruption of plastoglobule development, with the increased number of globules being a compensation mechanism. Previously, in herbicide (Norflurazon) treated wheat where phytoene desaturation was blocked enlarged phytoene containing plastoglobules occurred (Dahlin and Ryberg, 1986). Conversely the plastoglobules in transgenic floral plastids (Fig. 7) were much larger in size compared to the wild-type. This is likely related to the esterified nature of the non-endogenous

carotenoids in these tissues. In effect esterification appears to enable expansion of the plastoglubles which act as a sink for carotenoid sequestration, enabling significant increases in carotenoid accumulation in transgenic flowers, relative to wild type flowers. This may be due to the increased lipophilicity of carotenoid esters over their non-esterified counterparts and reflects the specialisation of chromoplasts to carotenoid accumulation. Changes in plastoglobule morphology in response to altered lipid content has been shown previously (Lundquist et al., 2013), where the loss of plastoglobule kinases (ABC1K1 and ABC1K3), resulted in modified prenyl-lipid composition of the plastoglobule. In addition to assisting sequestration, esterification also appears to confer greater stability to the carotenoid. Recently, the carotenoid cleavage dioxygenase (CCD4) has been should to act on β-ring carotenoids (Bruno et al., 2016), given the location of CCD4 in the plastogobule (Nacir and Brehelin, 2013; Ytterberg et al., 2006) it is likely that this enzyme will act on hydroxyl/keto carotenoids, but not when esterified, as in the plastoglobule the ratio of free to esterified carotenoids differs to that found in the membrane, with a greater abundance of esterified non-endogenous carotenoids present in the plastoglobule.

Analysis of photosynthetic complexes revealed that the non-endogenous ketocarotenoids were predominantly membrane components with only low levels associated with the photosynthetic complexes (Table 3). Carotenoids, especially xanthophylls are vital components of the photosynthetic apparatus in higher plants (Frank and Cogdell, 1996) and have been shown to be essential for the stable assembly of pigment–protein complexes (Green and Durnford, 1996). Previously, a lack of wild type carotenoid composition in xanthophylls biosynthetic mutants of *A. thaliana* (Gilmore, 2001) and an ε-ring carotenoid free mutant of *Scenedesmus obliquus* (Bishop, 1996), have led to an instability of trimeric LHCII and a reduction in PSII efficiency. Although a reduction in LHCII trimer stability and photosynthetic activity was witnessed in this study, it was β-ring carotenoids that were replaced by ketocarotenoids not ε-ring carotenoids (such as lutein) in photosynthetic complexes. Therefore, these findings seem to be in agreement with the recent findings for ketocarotenoid producing tobacco leaves (Röding et al 2015) that propose perturbations to the lipid phase of the thylakoids reducing photosystem stability. Despite the clear changes in carotenoid composition (Table 1), alterations in plastid ultrastructure (Figs. 6 and 7), changes to photosynthetic complexes (Table 3; Fig. 5) and photosynthetic efficiency, no significant changes in the transcript of the biosynthetic pathway genes were observed (Supplemental Table S4). This is surprising considering perturbations at the transcriptional level have been reported as a result of altered intermediate and end-product carotenoids (Giuliano et al., 1993).

To assess the effects the formation of these ketocarotenoids across metabolism, metabolite profiling was carried out. From the metabolite profiles it is clear that the transgenic *crtZ/W* lines are

not substantially equivalent to the wild type. However, the metabolites contributing to the greatest variance in composition were predominately well characterized primary metabolites (Table 4). These data suggest that the presence of ketocarotenoids directly affects metabolite composition. The reduction in amino acids derived from pyruvate in leaves could reflect the rapid utilization of pyruvate through the Methylerythritol 4-phosphate (MEP) pathway in chloroplasts. In contrast the increased levels in petals could reflect the different partitioning of intermediary carbon metabolism in sink tissues.

CONCLUSION

Significant levels of valuable ketocarotenoids have been produced in this study by transcriptional and translationally-enhanced *Brevundimonas CrtZ*/*W*, both in vegetative and flower tissues. In addition to astaxanthin and canthaxanthin, other rare keto/hydroxylated carotenoids have been produced, including a new ketocarotenoid elucidated in the flower tissue. The bioactivity of these compounds awaits testing. Although the levels present are not as high as those found with transplastomic tobacco varieties (Hasunuma et al., 2008), lettuce (Harada et al., 2014) or the extraordinary levels reported in tomato (Huang et al., 2013), the present study extends the range of hosts amenable to ketocarotenoid production and in a crop that can be used for biorefining feedstock, as it grows on marginal lands and has biofuel potential (Mortimer et al., 2012). The development of assessment of a multi-fractional refining cascade for *N.glauca* derived material is now important to enable the exploitation of complementary chemistries including nicotine-like compounds such as anabasine for use as insecticides. The present study has also provided valuable insights into the fundamental aspects of how plant cells sequestrate novel products generated from engineered biosynthetic capabilities. The metabolite profiling and transcriptional analysis of the target pathway suggest that the host have the metabolic plasticity to cope with the synthesis of these non-endogenous compounds. Interestingly, the most obvious perturbations appear to be at the structural level with the alterations in sub-plastidial components. Therefore, the cell reacts to changes in chemical composition by adopting or adjusting its cellular structures. These are changes at the cellular level, arising from perturbations in chemical composition, not predefined cellular structures waiting to be packaged with defined metabolites.

MATERIALS AND METHODS

Biological Materials and Growth Conditions

Agrobacterium tumefaciens strain LBA4404 was used to infect tobacco plants. Plasmid pUTR-crtZW(pZK3B) was transformed into *A. tumefaciens* by electroporation. *Nicotiana tabacum* cv. Sansum, and *Nicotiana glauca* and grown in 30 cm diameter pots containing Scotts® Levington® professional growing medium M2 (http://scottsprofessional.co.uk/uk/m2.html). Plants were glasshouse-grown with a daytime temperature of 20-25°C and nocturnal temperature of 15°C. Plants were grown in a 16 h supplementary light and 8 h darkness cycle.

Construction of Vectors for *N. glauca* Transformations

The *crtW* and *crtZ* genes, encoding CRTW and CRTZ proteins from *Brevundimonas* sp. strain SD-212, respectively, were chemically synthesized according to the codon usage of rape (*Brassica napus*) The synthetic *crtW* and *crtZ* genes (GenBank accession no. AB377271 andAB377272, respectively) were utilized in previous studies (Hasunuma et al.,(2008; Fujisawa et al., (2009). Plasmids were constructed according to standard methods (Sambrook et al., 1989). To import the gene products into plastids, a DNA fragment encoding the transit peptide (tp) of ribulose 1,5-bisphosphate carboxylase/oxygenase (RuBisCO) small subunit from pea was fused to the 5' end upstream of each open reading frame (ORF) (Misawa et al., 1993). In order to increase translational levels of the genes, the 5'-untranslated region (UTR) of the *N. tabacum* alcohol dehydrogenase gene (*NtADH*) was attached to the ATG of each gene, preceded with the transit peptide sequence (Satoh et al., 2004). Each gene cassette was constructed by connecting its gene construct between the cauliflower mosaic virus 35S (CaMV 35S) promoter (P_{35S}) and the *Arabidopsis* heat shock protein 18.2 gene (*HSP*) terminator (T_{HSP}) or an *HSP-nos* double terminator (DT2). This *HSP* terminator has been reported to support increased levels of the expression of a foreign gene (Nagaya et al., 2010). The resultant P_{35S}-UTR-tp-*crtZ*-DT2 and P_{35S}-UTR-tp-*crtW*-T_{HSP} cassettes were cloned with *E. coli* vector pUC198AM, which includes the pUC19 multiple cloning sites flanked with *Asc*I and *Mlu*I (Kuroda et al., 2010). Kuroda et al (2010) also constructed a binary vector pZK3B, a derivative of the plasmid pPZP202 (Hajdukiewicz et al., 1994). This vector features kanamycin resistance (Km^r) bacterial marker genes for selection of recombinant plants and a spectinomycin resistance ($spec^r$) bacterial marker gene for selection of recombinant bacteria. The *Asc*I- P_{35S}-UTR-tp-*crtZ*-DT2-*Mlu*I and *Asc*I- P_{35S}-UTR-tp- *crtW*-T_{HSP}-*Mlu*I fragments were cut out, and tandem inserted into the *Asc*I site of pZK3B, creating the desired plasmid pUTR-crtZW(pZK3B) (Supplemental Fig. 2).

Generation of Transgenic Plants

Agrobacterium-mediated transformation of *N.glauca* and its regeneration were carried out as described by Horsch et al. (1985). *N. glauca* seeds, collected from self pollinated T_0 plants, were sterilised and sown on MS agar media, supplemented with kanamycin (100 μg mL^{-1}). After three weeks' growth, segregation analysis was used to identify single insertion events. Germinated seedlings were scored for kanamycin sensitivity. Where the segregation of these groups was consistent with that of Mendelian inheritance, the seed was determined to be from a plant with a single insertion event. Seedlings with a score of 0 were deemed azygous, a score of 1 hemizygous and a score of 2 homozygous. The copy number of the transgenes in homozygous plants was subsequently established by qPCR.

DNA and RNA Isolation and Quantitative Analysis

Total plant DNA was isolated using the DNeasy mini kit (Qiagen). RNA was extracted using the RNeasy reagents and protocol, including on-column DNaseI digestion (Qiagen). The Rotor-gene SYBR Green RT-PCR Kit was used to determine gene expression levels and Rotor-Gene™ SYBR® Green PCR Kit (Qiagen) used to determine transgene copy number. Analysis of copy number relied upon the relative amplification of the transgenes and an endogenous single-copy gene, phytoene desaturase (*Pds).* Per reaction, 25 ng of RNA or DNA, was used and primers added to provide a final concentration of 2 μM in a final reaction volume of 25 μL. Reactions were performed on a Rotor-Gene 3000 thermocycler (Corbett Life Science). Thermocycling conditions for qRT-PCR were 10 min at 55°C for reverse transcription, 5 min at 95°C, followed by 40 cycles of 5 sec at 95°C, 10 sec at 60°C. Thermocycling conditions for qPCR were 5 min at 55°C for PCR activation, followed by 35 cycles of 5 sec at 95°C and 10 sec at 60°C for PCR amplification. Melt curve analysis verified specificity. Quantification and calibration curves were run simultaneously with experimental samples, and Ct calculations were performed by the Rotor-Gene software (Corbett Life Science). The actin gene served as reference for normalization for qRT-PCR. For qPCR, relative quantification by standard curves enabled direct relation of Ct signals of target transgenes to the Ct signal of the single copy calibrator; *Pds*. Samples with half the relative concentration of the calibrator were deemed hemizygous. Samples with the same relative concentration were deemed homozygous for one copy of the transgene (Bubner and Baldwin, 2004). All reactions were run in triplicate. Primers were designed using Primer3 software (http://primer3.sourcetorge.net/) and are shown in Supplemental Table S5.

Pigment Extraction and Analysis

The extraction, HPLC separation, photodiode array detection and quantification of carotenoids have been described in detail previously (Fraser et al., 2000). Plant material was frozen on collection or after treatment and freeze dried. Freeze dried tissue was ground to a fine powder with a Tissuelyser (Qiagen) at 30Hz. Extractions were made from 10-20 mg samples of leaf and flower tissue or 200 mg samples of tuber tissue in 1.5 mL micro-centrifuge tubes. Carotenoids and chlorophylls were extracted using chloroform and methanol (2:1), stored for 60 min on ice and 1 vol of water added. The organic hypophase was removed and the aqueous phase re-extracted with chloroform (2 by vol). Pooled extracts were dried under nitrogen gas. The residue was re-suspended in ethyl acetate (50 µL). HPLC separations were performed using C_{30} reverse-phase columns purchased from YMC. For screening analysis the mobile phases used were methanol (A), water/methanol (20/80 by vol), containing 0.2% ammonium acetate (B), and tert-methyl butyl ether (C). The gradient was 95% A: 5% B, isocratically for 2 min, stepped to 80% A: 5% B: 15% C, from which a linear gradient to 30% A: 5%B:65% C over 23 min was performed. For detailed analysis mobile phases used were methanol (A), water/methanol (50/50 by volume), containing 0.2% ammonium acetate (B), and tert-methyl butyl ether (C). The gradient was 95% A: 5%B, isocratically for 6 min, stepped to 80% A: 5% B: 15% C, from which a linear gradient to 30% A: 5% B: 65% C over 42 min was performed. A Waters Alliance HPLC system was used (600S controller, 610 pump, 996 photodiode array detector and 717plus autosampler). Detection was performed continuously from 220 to 700 nm with an online photodiode array detector. Identification was performed by co-chromatography and comparison of spectral properties and retention times with authentic standards (Sima-Aldrich and CaroNature Co.) and reference spectra (Britton et al., 2004). Carotenoid esters were identified as compounds with carotenoid or ketocarotenoid like spectra, with delayed retention times. Quantitative determination of carotenoids was performed by comparison with individual dose–response curves (0.2 to 1.5 µg) constructed from authentic standards. Structural elucidation of carotenoids was assisted where necessary by analyzing both the spectral absorption and mass spectra of carotenoid extracts. MS analysis was carried out using a high resolution Q-TOF mass spectrometer UHR-MAXIS (Bruker Daltonics), on-line with a UHPLC UltiMate 3000 equipped with a PDA detector (Dionex Softron). Chromatographic separations were performed in a similar manner to previously detailed Fraser et al 2000, with the exception that a RP C_{30} 3 µm column (150 x 2.1 mm i.d.) coupled to a 20 x 4.6 mm C_{30} guard column was used (YMC Inc.). The mobile phase was altered to facilitate ionisation and was comprised of (A) methanol, containing 0.1% formic acid and (B) *tert*-butyl methyl ether, containing 0.1% formic acid. These solvents were used in a gradient mode starting at 100% (A) for 5 min, then stepped to 95% (A) for 1 min, held it for 4 min and followed by a linear gradient over 30 min to 10% (A). This last condition was kept for 10 min in isocratic mode and after that initial conditions (100% A) were restored for 2 min. The column was

then re-equilibrated for 5 min. The flow rate used was 0.2 ml/min and the injection volume was 10 µl. The positive ionisation mode was atmospheric pressure chemical ionisation (APCI). Capillary and APCI vaporisation temperatures were 200 °C and 450 °C, respectively and the dry gas (nitrogen) and nebulizer were set at 3 l/min and 3 bar, respectively. APCI source settings were: corona discharge voltage at 4000 nA and a capillary voltage of 4 kV. A full MS scan was performed from 100 to 1600 *m/z* and MS/MS spectra were recorded at an isolation width of 0.5 *m/z*. Instrument calibration was performed externally prior to each sequence with APPI/APCI calibrant solution (Agilent Technologies). Automated post-run internal calibration was performed by injecting the same APPI/APCI calibrant solution at the end of each sample run via a six port divert valve equipped with a 20 µl loop.

The structure of the novel carotenoid 3-hydroxy-epoxyechinenone was derived from its spectral and mass data and obtained as detailed above. Additionally, a shift in spectral characteristics following reduction with $NaBH_4$ and colour-change from orange/red to green after acid hydrolysis with trifluoroacetic acid vapour was consistent with the presence of a keto and monoepoxide groups, respectively (Britton et al., 2004).

Analyses of Leaf Tissue

ΔE^*ab, as a measure of leaf color on the Hunter Lab Colour scale, was calculated from the color parameters *L, b* and *a* as measured with a MiniScan® XE plus (HunterLab). *In vivo* chlorophyll fluorescence was determined using a pocket PEA (plant efficiency analyzer) chlorophyll fluorimeter (http://www.hansatech-instruments.com/pocketPea.htm). Measurements were recorded with attached leaves. Fluorescence parameters are according to Vankooten and Snel (1990). $F_v/F_m = (F_m-F_0)/ F_m$ is the maximum photochemical efficiency of PS II, in the dark-adapted state.

Transmission electron microscopy (TEM) imaging service was provided by the Microscopy and Imaging Facility at the University of Kent (University of Kent, Canterbury, Kent, CT2 7NZ). Subsequent images were analysed with ImageJ software (National Institutes of Health (NIH), USA). The software was used to calculate total planar area of chloroplasts and the area occupied within chloroplasts by thylakoid membrane, starch granules and plastoglobule (PG) structures. The software enabled the measurement of surface areas by defining the spatial scale of the image using the scale bars on given TEM images. This enabled the measured areas to be presented in calibrated units. After scales were set, thylakoid grana, starch granules or PGs visible in the images were highlighted and their areas calculated using the 'Measure' function embedded in the software.

721 Grana were defined as thylakoid membrane structures more than two layers thick. Measurements
722 were exported to and analysed with Excel (Microsoft).
723 Plastids were isolated from WT and transgenic leaf tissue as detailed elsewhere (Anderson
724 et al., 1982). Separation of plastid components; plastoglobules, stroma and plastid/thylakoid
725 membrane, was performed as detailed in Ytterberg et al. (2006). Fractionation of chloroplasts on
726 sucrose gradients was performed as in Vidi et al. (2006). Fractions (2 mL) were collected, starting
727 at the top of sucrose gradients, prepared from three separate plastid preparations. Fractions from the
728 three separate gradients were pooled. Carotenoids were extracted from pooled fractions using
729 chloroform and methanol (2:1); following removal of the organic hypophase a volume of methanol,
730 equal to the organic phase removed, was added to concentrate proteins. Proteins were separated by
731 SDS-PAGE, and either stained by silver nitrate or blotted onto nitrocellulose membrane for
732 immunodetection. Blots were probed with a serum raised against plastoglobulin 35 (PGL35), PsbA
733 D1 protein of PSII, C terminal, RuBisCO large subunit (RbcL), chloroplast inner envelope
734 membrane translocon complex protein (TiC40), and chloroplast outer envelope membrane
735 translocon complex OEP75 protein (Agrisera), as directed by the manufacturer.
736 Partially denaturing ('green') gel electrophoresis isolation of pigment-protein complexes
737 was performed as in Dormann et al. (1995). Gels were not stained. For comparison of band intensity
738 samples of WT and transgenic solubilised pigment-protein complexes, representing 10 μg total
739 chlorophyll, were separated side by side on the same gels. Gels were scanned with a UMAX image
740 scanner (Amersham Biosciences) and images analysed with ImageJ software to calculate relative
741 band intensities. To enable sufficient pigment extraction from 'green' gels for detailed HPLC-PDA
742 analysis, solubilised pigment-protein complexes representing 250 μg total chlorophyll from their
743 respective tissues were separated. Pigment was extracted from isolated bands as detailed in Aizawa
744 et al. (1997).
745 Protein identification using LC-MS was carried out as described in Robertson et al 2012 and Mora
746 et al. (2013). Lanes containing bands of pigment protein complexes were excised from partially
747 denaturing gels. The proteins present were denatured in SDS loading buffer at 67°C for 5 minutes.
748 SDS-PAGE at 100V for 1 hr carried out and the resulting gels silver stained, using a ProteoSilver^{TM}
749 Plus Silver Stain Kit (Sigma-Aldrich). In-gel enzyme digestion for LC MS analysis was performed
750 as described in Robertson et al 2012. In-gel tryptic digests were filtered with PTFE syringe filters
751 (0.45μm), prior to nanoLC ESI MS/MS analysis. Nano-LC ESI MS/MS experiments were
752 performed on a AmaZon ETD Ion trap mass spectrometer (Brüker) connected to a nano-LC system
753 (Dionex U3000). Samples were loaded onto a 200μm i.d. x 5mm PepMap C18 RP trap column
754 (Dionex) with a flow rate of 4μl/minute of 0.1% FA, 2% ACN for 3 minutes. After pre-
755 concentration the trap column was automatically switched in-line with the PepMap analytical

column (2µm, 100µm id., 15cm, Dionex) and the peptides eluted with a linear gradient starting at 95 % eluent A (0.1 % formic acid in water) to 60 % of eluent B (0.1 % formic acid in 80 % acetonitrile) over 40 minutes, with a flow rate of 250nl/minute. Filtered in-gel digests were injected using a Dionex U3000 autosampler and Dionex U3000 nanoLC pumps. A nanoESI flow (Brüker) interface was used for the nanoESI. Ion spray voltage was set to 4.5 kV. Nitrogen was used as nebuliser gas at 15 psi, with dry gas at 5 l/minute at 220 °C. Helium was used as the collision gas. The AmaZon was run in enhanced resolution mode. The scan event cycle used a full scan mass spectrum from 350–1500 m/z and five corresponding data-dependent MS/MS events. HyStar 3.2, Data Analysis 4.0 and Biotools 3.0 software (Brüker) were employed for data analysis.

Statistical Analysis

Student's *t*-tests determined significant differences between pair-wise comparisons of wild type and transgenic samples. Student's *t*-tests, means, and standard error of the means (+/- SEM) were calculated using Excel software (Microsoft). Significance was determined when *t*-tests returned a p-value ≤ 0.05.

Accession Numbers

Sequence data from this article can be found in the EMBL/GenBank data libraries under accession numbers AB377271, AB377272 and X17295.

ACKNOWLEDGEMENTS

We thank Ian Brown at the Microscopy and Imaging Facility at the University of Kent, Canterbury, UK for carrying out the electron microscopy. Prof Sandmann, Frankfurt Universitat, is thanked for the supply of wild type *N.glauca* seeds and Mr Christopher Gerrish for skilled technical assistance during the execution of this work

SUPPLEMENTAL DATA

The following materials are available in the online version of this article.

Supplemental Figure S1. TLC separation of pigment extracts from leaf tissue of WT and *crtZ/crtW* transgenic *N. glauca*.

Lane 1, WT *N. glauca*. Lane 2, transgenic *N. glauca* line G1. Lane3, transgenic *N glauca* line G7. Region B1 contains β-carotene; B2 contains echinenone, chlorophyll and 3-OH-echinenone; B3 contains canthaxanthin, phoenicoxanthin, 4-ketozeaxanthin, astaxanthin, lutein and chlorophyll.

Supplemental Figure S2. Diagram of the pUTR-*crtZW* (pZK3B) plasmid

Supplemental Table S1. Analysis of T_0 and T_1 WT and *crtZ/crtW N. glauca* plants.

Supplemental Table S2. Chromatographic and spectral properties of pigments indentified in WT and *crtZ*/*crtW* transgenic *N. glauca* plant tissues.

Supplemental Table S3. MS/MS spectrometry identification of marker proteins isolated from photosynthetic complexes separated by partially denaturing 'green' gels electrophoresis.

Supplemental Table S4. Chlorophyll fluorescence and quantification in WT and transgenic *N.glauca*

Supplemental Table S5. qRT-PCR analysis of isoprenoid biosynthetic gene expression in WT and *crtW/crtZ* transgenic *N. glauca* tissue.

Supplemental Table S6. PCR primers used in the study.

FIGURE LEGENDS

Figure 1. Schematic illustration of the biosynthesis of astaxanthin from endogenous β-carotene, resulting from *Brevundimonas* sp. *crtW* and *crtZ* expression in *N. glauca* plants. Enzymes are indicated by their gene assignment symbols: CRTW, β-carotene ketolase; CRTZ, 3,3` hydroxylase coloured shading also indicates the functional groups introduced by these enzymes.

Figure 2. Colour changes in the flowers and aerial parts of transgenic T_0 *N. glauca* plants expressing *Brevundimonas* sp. *crtW* and *crtZ*.

(A) Wild type (WT)

(B) Senesced WT leaf

(C) WT flower. Ovary and nectary tissue are indicated by upper and lower arrows, respectively.

(D-E) Transgenic plants G1 and G7, respectively.

(F) Senesced leaf from transgenic plant G1

(G) G1 flower

Aerial phenotype in **(C)** is representative of all recombinant *N. glauca* plants, with the exception of line G7, shown in **(E)**. Floral phenotype in **(F)** is representative of all recombinant *N. glauca plants*. Bars = 4 cm for **(A) (D)** and **(E)**, 1cm for **(B) (F)**, and 0.5 cm for **(C)** and **(G)**.

Figure 3. HPLC-Photo diode array (PDA) profiles of carotenoids present in leaf and petal tissue from WT and *crtZ/crtW* transgenic *N. glauca* plants.

(A) WT leaf.

(B) *crtZ/crtW* transgenic leaf.

(C) WT petal.

(D) *crtZ/crtW t*ransgenic petal.

Each chromatogram component is labelled. Those labelled 11-20 (in bold) and KE (ketocarotenoid esters), were unique to transgenic plants. Component 19 in (B) was identified as a novel ketocarotenoid. See Supplemental Table S2 for spectral and chromatographic properties.

Figure 4. SDS-PAGE separation and immunoblot analysis of WT and *crtZ/crtW* transgenic, chloroplast fractions.

(A-B) SDS-Page separation of WT (A) and G1 (B) chloroplast fractions.

Total membranes from isolated chloroplasts were separated by flotation on a discontinuous sucrose gradient. Gradients were prepared from three separate plastid preparations. Fractions from the 3 separate gradients were pooled. Fractions 1 to 15 in addition to stromal preparations (ST) are indicated.

(C-D) Immunoblot analysis of WT (C) and G1 (D) chloroplast fractions.

Immunoblot analysis was performed using marker antibodies (Agrisera). PVDF membranes were probed successively with antisera raised against plastoglobulin 35 (PGL35, 35kDa); chloroplast inner envelope membrane translocon complex protein (TIC40, 40kDa); chloroplast outer envelope membrane translocon complex protein (TOC75, 75kDa): thylakoid-associated D1 protein of PSII, (PsbA, 38kDa) and the stromal large subunit of RuBisCO (RbcL, 52kDa).

(E-H) HPLC-PDA analysis of WT (E, F) and G1 (G, H) chloroplast fractions.

Viola, violaxanthin; Neo, Neoxanthin; Zea, Zeaxanthin. Values are the average of three replicates, from pooled fractions of three independent discontinues sucrose gradients. Error bars indicate +SEM.

(I) Schematic representation of the abundance of chloroplast ultrastructures throughout sucrose gradients. An increase in colour intensity in each bar represents an increase in the

abundance of the indicated structure, respective to the fractions in the panels above (E and H). (1) plastoglobules; (2) inner chloroplast envelope; (3) outer chloroplast envelope; (4) thylakoid membrane (grana); (5) starch granule; (6) ribosome; (7) stroma.

Figure 5. Distribution of carotenoids within photosynthetic complexes isolated from WT and *crtW/crtZ* transgenic *N. glauca* plastids.

(A) Partially denaturing 'green' gel, electrophoretic separation, of pigment-protein complexes from WT and transgenic plastid preparations.

(B) Pigment composition of isolated photosynthetic complexes. % compositions were calculated from total carotenoids extracted for each gel band and are the average of three values from complexes isolated from separate plastid preparations. Error bars indicate +SEM.

. CCI, core complex 1; CCII core complex II, LHCII monomer, monomeric form of light harvesting complex II; LHCII trimer, trimeric form of light harvesting complex II; LHCI light harvesting complex I, Zea, zeaxanthin: Viol, violaxanthin

Figure 6. Changes in leaf plastid ultrastructure resulting from the expression of *Brevundimonas* sp. *crtW* and *crtZ*.

(A) WT plastid.

(B) G1 plastid.

(C) WT plastoglobules.

(D) G1 plastoglobules.

S, starch granule; T, thylakoid membrane; PG, plastoglobule. Scale bars are indicated in each panel. Sections were prepared from transverse sections of three leaves; representative sections have been illustrated.

Figure 7. Changes in petal plastid ultrastructure resulting from the expression of *Brevundimonas* sp. *crtW* and *crtZ*.

(A) WT plastid.

(B) G1 plastid.

(C) WT plastoglobules

(D) G1 plastoglobules.

PG, plastoglobule. Scale bars are indicated in each panel. Sections were prepared from transverse sections of three flowers, representative sections have been illustrated.

Table 1. Carotenoids in leaves and flowers of wild-type and *crtZ/crtW* transgenic *N. glauca* (μg mg^{-1} dry weight)

	WT	G1	G7	G8
A. Mature leaf tissue				
Phytoene	0.01 ± 0.00 (<1)	0.08 ± 0.01 (2)	0.12 ± 0.02* (11)	0.01 ± 0.00 (<1)
Lutein	3.12 ± 0.21 (48)	1.54 ± 0.02* (31)	0.47 ± 0.07* (38)	2.97 ± 0.17 (50)
β-Carotene	1.14 ± 0.03 (18)	0.47 ± 0.04* (9)	0.16 ± 0.02* (13)	0.82 ± 0.04 (14)
cis-β- Carotene	0.13 ± 0.00 (2)	0.05 ± 0.00* (1)	0.03 ± 0.00* (2)	0.44 ± 0.23 (7)
Zeaxanthin	0.88 ± 0.02 (14)	0.32 ± 0.04* (6)	0.09 ± 0.13* (7)	0.21 ± 0.02* (4)
Antheraxanthin	0.16 ± 0.09 (2)	0.47 ± 0.04* (9)	0.04 ± 0.02 (4)	0.08 ± 0.03 (1)
Violaxanthin	1.00 ± 0.01 (16)	0.29 ± 0.18* (5)	0.10 ± 0.02* (8)	0.15 ± 0.04* (3)
4-Ketolutein	¤	1.04 ± 0.14¤ (20)	0.00 ± 0.00¤ (0)	0.46 ± 0.02¤ (8)
Echinenone	¤	0.29 ± 0.04¤ (6)	0.06 ± 0.01¤ (5)	0.25 ± 0.01¤ (4)
3-OH-Echinenone	¤	trace¤	trace¤	0.01 ± 0.00¤ (<1)
Canthaxanthin	¤	0.10 ± 0.01¤ (2)	0.03 ± 0.01¤ (2)	0.08 ± 001¤ (1)
Phoenicoxanthin	¤	0.04 ± 0.00¤ (1)	0.02 ± 0.00¤ (2)	0.09 ± 0.05¤ (2)
4-Ketozeaxanthin	¤	0.34 ± 0.02¤ (7)	0.08 ± 0.01¤ (7)	0.27 ± 0.03¤ (5)
Astaxanthin	¤	0.10 ± 0.00¤ (2)	0.04 ± 0.01¤ (3)	0.14 ± 0.01¤ (2)
Total non-keto carotenoid	6.44 ± 0.23 (100)	3.23 ± 0.27* (63)	1.01 ± 0.16* (81)	4.68 ± 0.35* (78)
Total ketocarotenoid	¤	1.91 ± 0.15¤ (37)	0.24 ± 0.03¤ (19)	1.30 ± 0.06¤ (22)
Total	6.44 ± 0.23 (100)	5.14 ± 0.37* (100)	1.24 ± 0.13* (100)	5.98 ± 0.41 (100)
B. Petal tissue				
Phytoene	0.05 ± 0.00 (2)	0.53 ± 0.06* (7)	0.37 ± 0.02* (7)	0.48 ± 0.04* (9)
Lutein	1.50 ± 0.12 (56)	0.23 ± 0.02* (3)	0.29 ± 0.01* (5)	0.15 ± 0.01* (3)
β-Carotene	0.66 ± 0.07 (24)	0.42 ± 0.05* (6)	0.44 ± 0.04* (8)	0.48 ± 0.07* (9)
Zeaxanthin	0.02 ± 0.00 (1)	0.02 ± 0.02 (<1)	0.00 ± 0.00* (0)	0.00 ± 0.00* (0)
Violaxanthin	0.45 ± 0.06 (17)	0.10 ± 0.04* (1)	0.13 ± 0.03* (2)	0.04 ± 0.01* (1)
4-Ketolutein	¤	0.17 ± 0.03¤ (2)	0.09 ± 0.02¤ (2)	0.08 ± 0.01¤ (2)
Echinenone	¤	0.09 ± 0.03¤ (1)	0.04 ± 0.00¤ (1)	0.14 ± 0.03¤ (3)
3-OH-Echineone	¤	0.02 ± 0.00¤ (0)	0.01 ± 0.00¤ (<1)	0.02 ± 0.00¤ (<1)
3'-OH-Echienone	¤	trace¤	0.02 ± 0.00¤ (<1)	0.00 ± 0.00¤ (0)
3-OH-Epoxy-echinenone	¤	0.48 ± 0.06¤ (7)	0.41 ± 0.02¤ (7)	0.47 ± 0.02¤ (9)
Canthaxanthin	¤	0.15 ± 0.02¤ (2)	0.09 ± 0.01¤ (2)	0.24 ± 0.09¤ (5)
Phoenicoxanthin	¤	0.32 ± 0.03¤ (4)	0.19 ± 0.01¤ (3)	0.22 ± 0.03¤ (4)
4-Ketozeaxanthin	¤	0.00 ± 0.00¤ (0)	0.03 ± 0.00¤ (1)	0.02 ± 0.00¤ (0)
Astaxanthin	¤	0.29 ± 0.03¤ (4)	0.19 ± 0.00¤ (3)	0.20 ± 0.02¤ (4)
Total Ketocarotenoid	¤	1.54 ± 0.19¤ (21)	1.08 ± 0.06¤ (20)	1.39 ± 0.12¤ (27)
Ketocarotenoid ester	¤	4.40 ± 0.29¤ (61)	3.21 ± 0.28¤ (58)	2.65 ± 0.21¤ (51)
Total ketocarotenoid + ester	¤	5.95 ± 0.48¤ (82)	4.28 ± 0.29¤ (78)	4.03 ± 0.14¤ (78)
Total non ketocarotenoid	2.70 ± 0.25 (100)	1.30 ± 0.18* (18)	1.23 ± 0.09* (22)	1.16 ± 0.05* (22)
Total	2.70 ± 0.25 (100)	7.25 ± 0.66* (100)	5.51 ± 0.34* (100)	5.20 ± 0.19* (100)
C. Ovary and nectary tissue				
Phytoene	0.03 ± 0.00 (1)	0.45 ± 0.01* (3)	0.46 ± 0.27 (3)	0.55 ± 0.04* (5)
Lutein	0.58 ± 0.01 (22)	0.17 ± 0.12* (1)	0.14 ± 0.02* (1)	0.14 ± 0.02* (1)
β-carotene	1.72 ± 0.07 (66)	1.81 ± 0.05 (11)	1.78 ± 0.06 (12)	1.40 ± 0.04 (13)
Zeaxanthin	0.05 ± 0.00 (2)	0.00 ± 0.00* (0)	0.00 ± 0.00* (0)	0.00 ± 0.00* (0)
Violaxanthin	0.24 ± 0.09 (9)	0.06 ± 0.00 (<1)	0.13 ± 0.04 (1)	0.08 ± 0.00 (1)
4-Ketolutein	¤	0.12 ± 0.02¤ (1)	0.10 ± 0.01¤ (1)	0.08 ± 0.04¤ (1)
Echinenone	¤	0.30 ± 0.01¤ (2)	0.40 ± 0.02¤ (3)	0.31 ± 0.02¤ (3)
3'-OH-Echienone	¤	0.05 ± 0.00¤ (<1)	0.06 ± 0.00¤ (<1)	0.05 ± 0.00¤ (0)
3-OH-Epoxy-echinenone	¤	0.54 ± 0.04¤ (3)	0.40 ± 0.02¤ (3)	0.15 ± 0.00¤ (1)
Canthaxanthin	¤	1.03 ± 0.02¤ (6)	1.05 ± 0.06¤ (7)	0.56 ± 0.02¤ (5)
Phoenicoxanthin	¤	0.88 ± 0.04¤ (5)	0.95 ± 0.05¤ (6)	0.42 ± 0.13¤ (4)
4-Ketozeaxanthin	¤	0.06 ± 0.00¤ (<1)	0.07 ± 0.00¤ (<1)	0.08 ± 0.00¤ (1)
Astaxanthin	¤	0.24 ± 0.01¤ (1)	0.22 ± 0.01¤ (1)	0.23 ± 0.02¤ (2)
Total ketocarotenoid	¤	3.22 ± 0.03¤ (20)	3.26 ± 0.19¤ (21)	1.87 ± 0.11¤ (18)
Ketocarotenoid ester	¤	10.75 ± 0.31¤ (65)	9.50 ± 0.57¤ (62)	6.34 ± 0.69¤ (61)

Total ketocarotenoid + ester	¤	13.97 ± 0.34¤ (85)	12.76 ± 0.29¤ (84)	8.21 ± 0.77¤ (79)
Total nonketocarotenoid	2.62 ± 0.11 (100)	2.49 ± 0.07 (15)	2.48 ± 0.31 (16)	2.17 ± 0.09 (21)
Total	2.62 ± 0.11 (100)	16.45 ± 0.29* (100)	15.24 ± 1.02* (100)	10.38 ± 0.86* (100)

Total carotenoid and ketocarotenoid contents were calculated as the sum of each carotenoid or ketocarotenoid, respectively, as determined by HPLC-PDA analysis. Values are the average of six measurements, comprised of three biological replicates in duplicate, ±SEM. * denotes a statistically significant difference to WT ($p<0.05$). ¤ denotes pigment unique to *crtZ*/*crtW* transgenic plants. Values in parenthesis are % compositions of accumulative carotenoid quantities.

Table 2. Pigment accumulation in progressing stages of WT and *crtW/crtW* transgenic T_0 *N. glauca* leaf development (μg/ mg dry weight)

	WT Expanding	**WT Mature**	**WT Senesced**	**G1 Expanding**	**G1 Mature**	**G1 Senesced**
Phytoene	0.06 ± 0.01 (0)	0.01 ± 0.00 (<1)	0.02 ± 0.00 (2)	0.20 ± 0.01* (3)	0.08 ± 0.01 (2)	0.40 ± 0.01* (30)
Lutein	3.04 ± 0.07 (45)	3.12 ± 0.21 (48)	0.48 ± 0.16 (51)	1.95 ± 0.08* (31)	1.54 ± 0.02* (31)	0.17 ± 0.03* (13)
β-Carotene	1.18 ± 0.11 (18)	1.14 ± 0.03 (18)	0.11 ± 0.01 (11)	0.73 ± 0.04* (11)	0.47 ± 0.04* (9)	0.09 ± 0.01 (7)
cis-β -Ccarotene	0.14 ± 0.01 (2)	0.13 ± 0.00 (2)	0.02 ± 0.01 (2)	0.09 ± 0.01* (1)	0.05 ± 0.00* (1)	0.03 ± 0.01* (2)
Zeaxanthin	1.54 ± 0.21 (23)	0.88 ± 0.02 (14)	0.13 ± 0.01 (13)	0.56 ± 0.13* (9)	0.32 ± 0.04* (6)	0.06 ± 0.02* (5)
Antheraxanthin	0.10 ± 0.04 (1)	0.16 ± 0.09 (2)	0.07 ± 0.01 (7)	0.80 ± 0.12* (12)	0.47 ± 0.04* (9)	0.14 ± 0.05 (10)
Violaxanthin	0.68 ± 0.10 (10)	1.00 ± 0.01 (16)	0.14 ± 0.02 (14)	0.16 ± 0.05* (2)	0.29 ± 0.18* (5)	0.01 ± 0.00* (<1)
4-Ketolutein	¤	¤	¤	0.73 ± 0.03¤ (11)	1.04 ± 0.14¤ (20)	0.01 ± 0.01¤ (1)
Echinenone	¤	¤	¤	0.30 ± 0.04¤ (5)	0.29 ± 0.04¤ (6)	0.03 ± 0.01¤ (2)
3-OH-Echinenone	¤	¤	¤	0.01 ± 0.00¤ (<1)	trace¤	0.00 ± 0.00¤ (0)
Canthaxanthin	¤	¤	¤	0.05 ± 0.00¤ (1)	0.10 ± 0.01¤ (2)	0.03 ± 0.01¤ (2)
Phoenicoxanthin	¤	¤	¤	0.11 ± 0.01¤ (2)	0.04 ± 0.00¤ (1)	0.00 ± 0.00¤ (0)
4-Ketozeaxanthin	¤	¤	¤	0.55 ± 0.03¤ (9)	0.34 ± 0.02¤ (7)	0.05 ± 0.02¤ (4)
Astaxanthin	¤	¤	¤	0.17 ± 0.03¤ (3)	0.10 ± 0.00¤ (2)	0.05 ± 0.02¤ (3)
Free ketocarotenoid	¤	¤	¤	1.91 ± 0.04¤ (30)	1.91 ± 0.15¤ (37)	0.17 ± 0.07¤ (13)
Ketocarotenoid ester	¤	¤	¤	0.00 ± 0.00 (0)	0.00 ± 0.00¤ (0)	0.27 ± 0.11¤ (20)
Total non-ketocarotenoid	6.74 ± 0.35 (100)	6.44 ± 0.23 (100)	0.96 ± 0.09 (100)	4.50 ± 0.41* (70)	3.23 ± 0.27* (63)	0.90 ± 0.10 (67)
Total	6.74 ± 0.35 (100)	6.44 ± 0.23 (100)	0.96 ± 0.09 (100)	6.41 ± 0.74 (100)	5.14 ± 0.37* (100)	1.34 ± 0.04 (100)
Chlorophyll (a + *b*)	5.59 ± 0.28	6.20 ± 0.16	0.74 ± 0.49	5.40 ± 0.29	6.19 ± 0.53	0.72 ± 0.66

Total carotenoid and ketocarotenoid contents were calculated as the sum of each carotenoid or ketocarotenoid, respectively, as determined by HPLC-PDA analysis. Values are the average of six measurements, comprised of three biological replicates in duplicate, ± SEM. * denotes a statistically significant difference to WT at the same developmental stage ($p<0.05$). ¤ denotes pigment unique to *crtZ/crtW* transgenic plants. Values in parenthesis are % compositions of accumulative carotenoid quantities. Chlorophyll quantities were determined by spectrophotometry.

Table 3. Distribution of carotenoids within photosynthetic complexes isolated from *N. glauca* plastids (%)

		Lutein	β-Carotene	Violaxanthin	Zeaxanthin	Echinenone	4-Ketolutein	Total pigment (µg)
CCI	WT	33 ± 2	67 ± 2	0 ± 0	0 ± 0	0 ± 0	0 ± 0	0.043 ± 0.010
	G1	9 ± 2	53 ± 2	0 ± 0	2 ± 2	35 ± 2	0 ± 0	0.010 ± 0.002
	G7	2 ± 2	53 ± 4	0 ± 0	5 ± 0	40 ± 2	0 ± 0	0.003 ± 0.004
LHCII trimer	WT	82 ± 4	1 ± 1	14 ± 4	2 ± 1	0 ± 0	0 ± 0	1.741 ± 0.423
	G1	80 ± 2	2 ± 1	6 ± 0	5 ± 1	1 ± 1	4 ± 1	0.496 ± 0.076
	G7	83 ± 3	1 ± 0	8 ± 1	3 ± 1	1 ± 0	5 ± 2	0.765 ± 0.042
CCII	WT	71 ± 2	15 ± 6	11 ± 8	3 ± 1	0 ± 0	0 ± 0	0.538 ± 0.218
	G1	60 ± 5	15 ± 1	0 ± 0	3 ± 2	16 ± 1	5 ± 2	0.123 ± 0.011
	G7	47 ± 3	12 ± 1	1 ± 1	7 ± 1	22 ± 2	11 ± 1	0.126 ± 0.027
LHC mono	WT	66 ± 2	3 ± 1	30 ± 3	1 ± 1	0 ± 0	0 ± 0	0.608 ± 0.247
	G1	80 ± 3	1 ± 0	8 ± 4	4 ± 2	1 ± 0	5 ± 3	0.687 ± 0.040
	ZW	75 ± 1	1 ± 0	8 ±1	5 ± 0	1 ± 0	11 ± 1	0.851 ± 0.226

% compositions were calculated from total carotenoids extracted from each gel band as determined by HPLC-PDA analysis. Values are the average of three measurements from separate plastid preparations ± SEM. . CCI, core complex 1; CCII core complex II, LHCII monomer, monomeric form of light harvesting complex II; LHCII trimer, trimeric form of light harvesting complex II; LHCI light harvesting complex I.

923

Table 4: Metabolite levels of *crtZ/crtW* transgenic *N. glauca* leaf (T_0)and petal (T_1) tissue relative to their respective controls

Metabolite		Main site of synthesis	Leaf G1	Leaf G7	Petal G1(HO)
Organic acids	Acetic acid	MC/CY	0.84±0.46	1.09±0.77	0.11±0.37
	Citric acid	MT	3.05±0.86	0.35±0.05	1.14±0.33
	Gluconic acid	CY	0.00±0.00	0.55±0.61	n/d
	Lactic acid	CY	0.59±0.15	0.93±0.21	0.64±0.30
	Malic acid	MT/CY	0.81±0.18	**0.07±0.38**	1.04±0.51
	Oxalic acid	CY	**0.22±0.05**	**0.34±0.08**	0.94±0.12
Phosphates	Phosphoric acid		1.87±0.29	0.92±0.02	**1.42±0.03**
Amino acids	Alanine	PL	**0.30±0.04**	**0.27±0.01**	1.43±0.26
	Asparagine	CY	0.07±0.05	0.10±0.07	2.07±1.12
	Aspartic acid	CY	1.30±0.19	**0.25±0.03**	**2.32±0.14**
	Isoleucine	PL	**0.11±0.01**	**0.48±0.02**	**1.84±0.26**
	Glycine	CY(PE)	**0.16±0.02**	**0.35±0.03**	0.91±0.14
	Phenylalanine	CY	**0.48±0.04**	**0.43±0.03**	**2.75±0.21**
	Proline	CY	2.47±0.30	0.08±0.08	**2.83±0.08**
	Threonine	PL	**0.27±0.03**	**0.24±0.03**	**2.08±0.14**
	Valine	PL	**0.12±0.01**	**0.39±0.02**	**2.29±0.02**
Fatty acids	Linolenic acid	CY	0.75±0.39	0.61±0.16	1.50±0.29
	Lauric acid	PL	n/d	n/d	0.72±0.13
	Oleic acid	CY	n/d	n/d	1.29±0.21
	Palmitic acid	PL	0.12±0.03	0.09±0.01	1.46±0.23
	Stearic acid	CY	1.20±0.30	**1.83±0.61**	0.80±0.07
Carbohydrates	Arabinofuranose	CY	**0.29±0.13**	**0.15±0.07**	1.15±0.20
	Arabinose	CY	0.58±0.21	**0.39±0.21**	1.88±0.52
	Fructose	CY	**0.48±0.09**	**0.47±0.05**	1.03±0.05
	Glucose	CY/PL	0.60±0.12	0.52±0.15	2.30±0.57
	Ribose	CY	**0.58±0.08**	1.24±0.18	0.55±0.11
	Starch	PL	**0.75±0.07**	-	-
	Talose	CY/PL	n/d	n/d	**7.08±1.69**
	D-Turanose	CY	**0.30±0.09**	**0.33±0.05**	**1.96±0.33**
	Unknown sugar		**0.18±0.04**	**0.24±0.04**	1.17±0.16
	Unknown sugar		n/d	n/d	1.22±0.10
Polyols	Glycerol	CY	**0.00±0.00**	0.35±0.25	0.80±0.43
	Inositol	CY	**0.61±0.06**	**0.22±0.01**	1.68±0.30
N-containing compounds	2-Piperidinecarboxylic acid		n/d	n/d	0.75±0.04
	Putrescine	CY	n/d	n/d	0.69±0.23
	Quinazoline		n/d	n/d	1.41±0.17
Isoprenoids	β-Sitosterol	CY	**3.39±0.94**	**8.50±1.05**	1.09±0.16
	Stigmasterol	CY	**5..51±1.57**	**3.89±0.99**	1.36±0.23
	α-Tocopherol	PL	n/d	n/d	0.35±0.06
	Tocopherol	PL	n/d	n/d	0.30±0.09
Phenolic compounds	p-Coumaric acid	CY	n/d	n/d	0.66±0.13
	Ferulic acid	CY	**13.90±0.20**	**0.00±0.00**	1.71±0.12
	Kaempferol-3-O-rutinoside	CY	1.05±0.06	0.79±0.08	0.71±0.06
	Rutin	CY	**0.77±0.03**	**2.07±0.25**	0.38±0.17
Alkanes	C-Hentriacontane		**2.03±0.66**	**5.88±1.26**	2.74±0.90
	C-Heptacosane		n/d	n/d	0.70±0.06
	C-Nonacosane		n/d	n/d	0.87±0.10

924

925 Data have been compiled from multiple analytical platforms as outlined in the Methods section.
926 Data have been normalized to sample weight and expressed relative to their wild type. Values are
927 represented as means +/- SEM. Values in bold denotes a statistically significant difference to WT
928 ($p<0.05$). G1HO- G1, homozygous tissue. n/d -not detected in one of the pair wise ratios. –

929 indicates not determined Abbreviations for the site of synthesis are MT-mitochondria, CY-cytosol,
930 Pl-plastid and PE-peroxisomes.
931
932

933
934

Parsed Citations

Aizawa K, Cunningham FX, Gantt E (1997) Enhanced recovery of chlorophyll and carotenoids with dextran-polyacrylamide gel electrophoresis. Anal Sci 13: 253-256
Pubmed: Author and Title
CrossRef: Author and Title
Google Scholar: Author Only Title Only Author and Title

Anderson B, Anderson JM, Ryrie IJ (1982) Transbilayer organization of the chlorophyll-proteins of spinach thylakoids. E J Biochem 123: 465-472
Pubmed: Author and Title
CrossRef: Author and Title
Google Scholar: Author Only Title Only Author and Title

Auldridge ME, McCarty DR, Klee HJ (2006) Plant carotenoid cleavage oxygenases and their apocarotenoid products. Curr Opin Plant Biol 9: 315-321
Pubmed: Author and Title
CrossRef: Author and Title
Google Scholar: Author Only Title Only Author and Title

Ausich RL (1997) Commercial opportunities for carotenoid production by biotechnology. Pure Appl Chem 69: 2169-2173
Pubmed: Author and Title
CrossRef: Author and Title
Google Scholar: Author Only Title Only Author and Title

Austin JR, 2nd, Frost E, Vidi PA, Kessler F, Staehelin LA (2006) Plastoglobules are lipoprotein subcompartments of the chloroplast that are permanently coupled to thylakoid membranes and contain biosynthetic enzymes. Plant Cell 18: 1693-1703
Pubmed: Author and Title
CrossRef: Author and Title
Google Scholar: Author Only Title Only Author and Title

Bishop NI (1996) The ß,?-carotenoid, lutein, is specifically required for the formation of the oligomeric forms of the light harvesting complex in the green alga, Scenedesmus obliquus. J Photoch PhotobiolB: Biology 36: 279-283
Pubmed: Author and Title
CrossRef: Author and Title
Google Scholar: Author Only Title Only Author and Title

Breithaupt DE (2007) Modern application of xanthophylls in animal feeding - a review. Trends in Food SciTechnol 18: 501-506
Pubmed: Author and Title
CrossRef: Author and Title
Google Scholar: Author Only Title Only Author and Title

Brehelin C, Kessler F, van Wijk KJ (2007) Plastoglobules: Versatile lipoprotein particles in plastids. Trends Plant Sci. 12: 260-266.
Pubmed: Author and Title
CrossRef: Author and Title
Google Scholar: Author Only Title Only Author and Title

Britton G, LiaaenJensen S, Pfander H (2004) Carotenoids Handbook. Birkhauser Verlag, Basel.
Pubmed: Author and Title
CrossRef: Author and Title
Google Scholar: Author Only Title Only Author and Title

Bruno M, Koschmjeder J, Wuest F, Schaub P, Fehling-Kaschek M, Timmer J, Beyer P, Al-Babili S (2016) Enzymatic study on AtCCD4 and AtCCD7 and their potential to form acyclic regulatory metabolites. J Exp Bot 67: 5993-6005.
Pubmed: Author and Title
CrossRef: Author and Title
Google Scholar: Author Only Title Only Author and Title

Bubner B, Baldwin IT (2004) Use of real-time PCR for determining copy number and zygosity in transgenic plants. Plant Cell Rep 23: 263-271
Pubmed: Author and Title
CrossRef: Author and Title
Google Scholar: Author Only Title Only Author and Title

Chamovitz D, Sandmann G, Hirschberg J (1993) Molecular and biochemical characterization of herbicide-resistant mutants of cyanobacteria reveals that phytoene desaturation is a rate-limiting step in carotenoid biosynthesis. J Biol Chem 268: 17348-17353
Pubmed: Author and Title
CrossRef: Author and Title
Google Scholar: Author Only Title Only Author and Title

Choi SK, Harada H, Matsuda S, Misawa N (2007) Characterization of two beta-carotene ketolases, crtO and crtW, by complementation analysis in Escherichia coli. Appl MicrobiolBiotechnol 75: 1335-1341
Pubmed: Author and Title
CrossRef: Author and Title
Google Scholar: Author Only Title Only Author and Title

Choi SK, Matsuda S, Hoshino T, Peng X, Misawa N (2006) Characterization of bacterial beta-carotene 3,3 '-hydroxylases, crtZ, and P450 in astaxanthin biosynthetic pathway and adonirubin production by gene combination in Escherichia coli. Appl Microbiol Biotechnol 72: 1238-1246
Pubmed: Author and Title

CrossRef: Author and Title
Google Scholar: Author Only Title Only Author and Title

Choi SK, Nishida Y, Matsuda S, Adachi K, Kasai H, Peng X, Komemushi S, Miki W, Misawa N (2005) Characterization of beta-carotene ketolases, crtW, from marine bacteria by complementation analysis in Escherichia coli. Marine Biotech 7: 515-522
Pubmed: Author and Title
CrossRef: Author and Title
Google Scholar: Author Only Title Only Author and Title

Cunningham FX, Gantt E (2005) A study in scarlet: enzymes of ketocarotenoid biosynthesis in the flowers of Adonis aestivalis. Plant J 41: 478-492
Pubmed: Author and Title
CrossRef: Author and Title
Google Scholar: Author Only Title Only Author and Title

Curt MD, Fernández J (1990) Production of Nicotiana glauca R.C. Graham aerial biomass in relation to irrigation regime. Biomass 23: 103-115
Pubmed: Author and Title
CrossRef: Author and Title
Google Scholar: Author Only Title Only Author and Title

Dahlin C, Ryberg H (1986) Accumulation of phytoene in plastoglobuli of SAN-9789 (Norflurazon)-treated dark-grown wheat. Physiol Plant 68: 39-45
Pubmed: Author and Title
CrossRef: Author and Title
Google Scholar: Author Only Title Only Author and Title

Dambeck M, Sandmann G (2014) Antioxidative activities of algal keto carotenoids acting as antioxidative protectants in the chloroplast. Photochem and Photobiol 90: 814-819
Pubmed: Author and Title
CrossRef: Author and Title
Google Scholar: Author Only Title Only Author and Title

Deruere J, Romer S, d'Harlingue A, Backhaus RA, Kuntz M, Camara B (1994) Fibril assembly and carotenoid overaccumulation in chromoplasts: a model for supramolecular lipoprotein structures. Plant Cell 6: 119-133
Pubmed: Author and Title
CrossRef: Author and Title
Google Scholar: Author Only Title Only Author and Title

Dormann P, Hoffmann-Benning S, Balbo I, Benning C (1995) Isolation and characterization of an Arabidopsis mutant deficient in the thylakoid lipid digalactosyl diacylglycerol. Plant Cell 7: 1801-1810
Pubmed: Author and Title
CrossRef: Author and Title
Google Scholar: Author Only Title Only Author and Title

Enfissi EMA, Nogueira M, Bramley PM, Fraser PD (2016) The regulation of carotenoid formtion in tomatofruit. The Plant J 10.111/tpj.13428
Pubmed: Author and Title
CrossRef: Author and Title
Google Scholar: Author Only Title Only Author and Title

Frank HA, Cogdell RJ (1996) Carotenoids in Photosynthesis. PhotochemPhotobiol 63: 257-264
Pubmed: Author and Title
CrossRef: Author and Title
Google Scholar: Author Only Title Only Author and Title

Fraser PD, Pinto MES, Holloway DE, Bramley PM (2000) Application of high-performance liquid chromatography with photodiode array detection to the metabolic profiling of plant isoprenoids. Plant J 24: 551-558
Pubmed: Author and Title
CrossRef: Author and Title
Google Scholar: Author Only Title Only Author and Title

Fraser PD, Shimada H, Misawa N (1998) Enzymatic confirmation of reactions involved in routes to astaxanthin formation, elucidated using a direct substrate in vitro assay. Eur J Biochem 252: 229-236
Pubmed: Author and Title
CrossRef: Author and Title
Google Scholar: Author Only Title Only Author and Title

Fraser PD, Truesdale MR, Bird CR, Schuch W, Bramley PM (1994) Carotenoid biosynthesis during tomato fruit-development. Plant Physiol 105: 405-413
Pubmed: Author and Title
CrossRef: Author and Title
Google Scholar: Author Only Title Only Author and Title

Fujisawa M, Takita E, Harada H, Sakurai N, Suzuki H, Ohyama K, Shibata D, Misawa N (2009) Pathway engineering of Brassica napus seeds using multiple key enzyme genes involved in ketocarotenoid formation. J Exp Bot 60: 1319-1332
Pubmed: Author and Title
CrossRef: Author and Title
Google Scholar: Author Only Title Only Author and Title

Gerjets T, Sandmann G (2006) Ketocarotenoid formation in transgenic potato. J Exp Bot57: 3639-3645

Pubmed: Author and Title
CrossRef: Author and Title
Google Scholar: Author Only Title Only Author and Title

Gerjets T, Sandmann M, Zhu C, Sandmann G (2007) Metabolic engineering of ketocarotenoid biosynthesis in leaves and flowers of tobacco species. Biotechnol J 2: 1263-1269
Pubmed: Author and Title
CrossRef: Author and Title
Google Scholar: Author Only Title Only Author and Title

Gilmore AM (2001) Xanthophyll cycle-dependent nonphotochemical quenching in Photosystem II: Mechanistic insights gained from Arabidopsis thaliana L. mutants that lack violaxanthin deepoxidase activity and/or lutein. Photosynth Res 67: 89-101
Pubmed: Author and Title
CrossRef: Author and Title
Google Scholar: Author Only Title Only Author and Title

Giuliano G, Bartley GE, Scolnik PA (1993) Regulation of carotenoid biosynthesis during tomato development. Plant Cell 5: 379-387
Pubmed: Author and Title
CrossRef: Author and Title
Google Scholar: Author Only Title Only Author and Title

Green BR, Durnford DG (1996) The chlorophyll-carotenoid proteins of oxygenic photosynthesis. Annu Rev Plant Physiol Plant Mol Biol 47: 685-714
Pubmed: Author and Title
CrossRef: Author and Title
Google Scholar: Author Only Title Only Author and Title

Hajdukiewicz P, Svab Z, Maliga P (1994) The small, versatile Ppzp family of Agrobacterium binary vectors for plant transformation. Plant Mol Biol 25: 989-994
Pubmed: Author and Title
CrossRef: Author and Title
Google Scholar: Author Only Title Only Author and Title

Harada H, Maoka T, Osawa A, Hattan J-i, Kanamoto H, Shindo K, Otomatsu T, Misawa N (2014) Construction of transplastomic lettuce (Lactuca sativa) dominantly producing astaxanthin fatty acid esters and detailed chemical analysis of generated carotenoids. Transgenic Res 23: 303-315
Pubmed: Author and Title
CrossRef: Author and Title
Google Scholar: Author Only Title Only Author and Title

Hasunuma T, Miyazawa SI, Yoshimura S, Shinzaki Y, Tomizawa KI, Shindo K, Choi SK, Misawa N, Miyake C (2008) Biosynthesis of astaxanthin in tobacco leaves by transplastomic engineering. Plant J 55: 857-868
Pubmed: Author and Title
CrossRef: Author and Title
Google Scholar: Author Only Title Only Author and Title

Havaux M, Dall'osto L, Bassi R (2007) Zeaxanthin has enhanced antioxidant capacity with respect to all other xanthophylls in Arabidopsis leaves and functions independent of binding to PSII antennae. Plant Physiol 145: 1506-1520
Pubmed: Author and Title
CrossRef: Author and Title
Google Scholar: Author Only Title Only Author and Title

Horsch RB, Fry JE, Hoffmann NL, Eichholtz D, Rogers SG, Fraley RT (1985) A simple and general-method for transferring genes into plants. Science 227: 1229-1231
Pubmed: Author and Title
CrossRef: Author and Title
Google Scholar: Author Only Title Only Author and Title

Huang J-C, Zhong Y-J, Liu J, Sandmann G, Chen F (2013) Metabolic engineering of tomato for high-yield production of astaxanthin. Metabol Eng 17: 59-67
Pubmed: Author and Title
CrossRef: Author and Title
Google Scholar: Author Only Title Only Author and Title

Jayaraj J, Devlin R, Punja Z (2008) Metabolic engineering of novel ketocarotenoid production in carrot plants. Transgenic Res 17: 489-501
Pubmed: Author and Title
CrossRef: Author and Title
Google Scholar: Author Only Title Only Author and Title

Josse E, Simkin AJ, Gaffe J, Laboure A, Kuntz M, Carol P (2000) A plastid terminal oxidase associated with carotenoid desaturation during chromoplast differentiation. Plant Physiol.123: 1427-1436.
Pubmed: Author and Title
CrossRef: Author and Title
Google Scholar: Author Only Title Only Author and Title

Kuroda M, Kimizu M, Mikami C (2010) A simple set of plasmids for the production of transgenic plants. Biosci Biotechnol Biochem 74: 2348-2351
Pubmed: Author and Title
CrossRef: Author and Title
Google Scholar: Author Only Title Only Author and Title

Latari K, Wuest F, Huebner M, Shaub P, Beisel KG, Matsubara S, Beyer P, Welsch R (2015) Tissue-speciifc Apocarotenoid glycosylation contributes to carotenoid homeostasis in Arabidopsis leaves. Plant Physio. 168: 1550-1562.
Pubmed: Author and Title
CrossRef: Author and Title
Google Scholar: Author Only Title Only Author and Title

Li L, Yang Y, Xu Q, Owsiany K, Welsch R, Chitchumroonchokchai C, Lu S, Van Eck J, Deng XX, Failla M, Thannhauser TW (2012) The Or gene enhances carotenoid accumulation and stability during post-harvest storage of potato tubers. Mol Plant 5: 339-352
Pubmed: Author and Title
CrossRef: Author and Title
Google Scholar: Author Only Title Only Author and Title

Lippold F, vom Dorp K, Abraham M, Hölzl G, Wewer V, Yilmaz JL, Lager I, Montandon C, Besagani C, Kessler F, Styme S, Dörmann P. (2012). Fatty acid phytyl ester synthesis in chloroplasts of Arabiodopsis. Plant Cell 24: 2001- 2014.
Pubmed: Author and Title
CrossRef: Author and Title
Google Scholar: Author Only Title Only Author and Title

Lorenz RT, Cysewski GR (2000) Commercial potential for Haematococcus microalgae as a natural source of astaxanthin. Trends in Technol 18: 160-167
Pubmed: Author and Title
CrossRef: Author and Title
Google Scholar: Author Only Title Only Author and Title

Lokstein H; Tian L; Polle JEW; DellaPenna, D (2002) Xanthophyll biosynthetic mutants of Arabidopsis thaliana: altered nonphotochemical quenching of chlorophyll fluorescence is due to changes in Photosystem II antenna size and stability. Biochem Biophys Acta-Bioenergetics 1553: 309-319
Pubmed: Author and Title
CrossRef: Author and Title
Google Scholar: Author Only Title Only Author and Title

Lundquist PK, Poliakov A, Giacomelli L, Friso G, Appel M, McQuinn RP, Krasnoff SB, Rowland E, Ponnala L, Sun Q, van Wijk KJ (2013) Loss of plastoglobule kinases ABC1K1 and ABC1K3 causes conditional degreening, modified prenyl-lipids and recuritment of the jasmonic acid pathway. The Plant Cell 25: 1818-1839.
Pubmed: Author and Title
CrossRef: Author and Title
Google Scholar: Author Only Title Only Author and Title

Matile P (2000) Biochemistry of Indian summer: physiology of autumnal leaf coloration. Exp Gerontol 35: 145-158
Pubmed: Author and Title
CrossRef: Author and Title
Google Scholar: Author Only Title Only Author and Title

Misawa N, Satomi Y, Kondo K, Yokoyama A, Kajiwara S, Saito T, Ohtani T, Miki W (1995) Structure and functional-analysis of a marine bacterial carotenoid biosynthesis gene-cluster and astaxanthin biosynthetic-pathway proposed at the gene level. JBacteriol 177: 6575-6584
Pubmed: Author and Title
CrossRef: Author and Title
Google Scholar: Author Only Title Only Author and Title

Misawa N, Yamano S, Linden H, Felipe MR, Lucas M, Ikenaga H, Sandmann G (1993) Functional expression of the Erwinia uredovora carotenoid biosynthesis gene crtI in transgenic plants showing an increase of beta-carotene biosynthesis activity and resistance to the bleaching herbicide norflurazon. Plant J 4: 833-840
Pubmed: Author and Title
CrossRef: Author and Title
Google Scholar: Author Only Title Only Author and Title

Mora L, Bramley PM, Fraser PD (2013) Development and optimisation of a label-free quantitative proteomic procedure and its application in the assessment of genetically modified tomato fruit. Proteomics 13: 2016-2030
Pubmed: Author and Title
CrossRef: Author and Title
Google Scholar: Author Only Title Only Author and Title

Morris WL, Ducreux LJM, Fraser PD, Millam S, Taylor MA (2006) Engineering ketocarotenoid biosynthesis in potato tubers. Metab Eng 8: 253-263
Pubmed: Author and Title
CrossRef: Author and Title
Google Scholar: Author Only Title Only Author and Title

Mortimer CL, Bramley PM, Fraser PD (2012) The identification and rapid extraction of hydrocarbons from Nicotiana glauca: A potential advanced renewable biofuel source. Phytochem Lett 5: 455-458
Pubmed: Author and Title
CrossRef: Author and Title
Google Scholar: Author Only Title Only Author and Title

Nacir H, Brehelin C (2013) When proteomics reveals unsuspected roles: The plastoglobule example. Front Plant Sci. 4: 114.
Pubmed: Author and Title
CrossRef: Author and Title
Google Scholar: Author Only Title Only Author and Title

Nagaya S, Kawamura K, Shinmyo A, Kato K (2010) The HSP terminator of Arabidopsis thaliana increases gene expression in plant cells. Plant Cell Physiol 51: 328-332
Pubmed: Author and Title
CrossRef: Author and Title
Google Scholar: Author Only Title Only Author and Title

NNFCC (2011) Advanced Biofuels: NNFCC's 19th Newsletter. In. The UK's National Centre for Biorenewable Energy, Fuels and Materials, York
Pubmed: Author and Title
CrossRef: Author and Title
Google Scholar: Author Only Title Only Author and Title

Nogueira M, Mora L, Enfissi EM, Bramley PM, Fraser PD (2013) Subchromoplast sequestration of carotenoids affects regulatory mechanisms in tomato lines expressing different carotenoid gene combinations. Plant Cell 25: 4560-4579
Pubmed: Author and Title
CrossRef: Author and Title
Google Scholar: Author Only Title Only Author and Title

Norris SR, Barrette TR, DellaPenna D (1995) Genetic dissection of carotenoid synthesis in Arabidopsis defines plastoquinine as an essential component of phytoene desaturation.Plant Cell 7: 2139-2149
Pubmed: Author and Title
CrossRef: Author and Title
Google Scholar: Author Only Title Only Author and Title

Park KM, Song MW, Lee JH (2009) Determination of kinetic parameters of growth and carotenogenesis in the red yeast Xanthophyllomyces dendrorhous. Biotechnol Bioprocess Eng 14: 414-418
Pubmed: Author and Title
CrossRef: Author and Title
Google Scholar: Author Only Title Only Author and Title

Robertson FP, Koistinen PK, Gerrish C, Halket JM, Patel RKP, Fraser PD, Bramley PM. 2012.
Pubmed: Author and Title
CrossRef: Author and Title
Google Scholar: Author Only Title Only Author and Title

Proteome changes in tomato lines transformed with phytoene synthase-1 in the sense and antisense orientations: J. Exp Bot. 63: 6035-6043.
Pubmed: Author and Title
CrossRef: Author and Title
Google Scholar: Author Only Title Only Author and Title

Röding A, Dietzel L, Schlicke H, Grimm B, Sandmann G and Büchel (2015) Production of ketocarotenoids in tobacco alters the photosynthetic efficiency by reducing photosytem II supercomplex and LHCII trimer stability. Photosynthetic Research 123: 157-165.
Pubmed: Author and Title
CrossRef: Author and Title
Google Scholar: Author Only Title Only Author and Title

Sambrook J, Fritsch EF, Maniatis T (1989) Molecular cloning: A labratory manual. Cold Spring Harbour Labratory Press, New York, USA
Pubmed: Author and Title
CrossRef: Author and Title
Google Scholar: Author Only Title Only Author and Title

Simkin AJ, Gaffe J, Alcaraz JP, Carde JP, Bramley PM, Fraser PD, Kuntz M (2007) Fibrillin influence on plastid ultrastructure and pigment content in tomato fruit. Phytochem 68: 1545-1556
Pubmed: Author and Title
CrossRef: Author and Title
Google Scholar: Author Only Title Only Author and Title

Thomas H, Huang L, Young M, Ougham H (2009) Evolution of plant senescence. BMC Evol Biol 9: 163
Pubmed: Author and Title
CrossRef: Author and Title
Google Scholar: Author Only Title Only Author and Title

Vankooten O, Snel JFH (1990) The use of chlorophyll fluorescence nomenclature in plant stress physiology. Photosyn Res 25: 147-150
Pubmed: Author and Title
CrossRef: Author and Title
Google Scholar: Author Only Title Only Author and Title

Vidi PA, Kanwischer M, Baginsky S, Austin JR, Csucs G, Dormann P, Kessler F, Brehelin C (2006) Tocopherol cyclase (VTE1) localization and vitamin E accumulation in chloroplast plastoglobule lipoprotein particles. JBiol Chem 281: 11225-11234
Pubmed: Author and Title
CrossRef: Author and Title
Google Scholar: Author Only Title Only Author and Title

Ytterberg AJ, Peltier J-B, van Wijk KJ (2006) Protein profiling of plastoglobules in chloroplasts and chromoplasts. A surprising site for differential accumulation of metabolic enzymes. Plant Physiol 140: 984-997
Pubmed: Author and Title

CrossRef: Author and Title
Google Scholar: Author Only Title Only Author and Title

Zhu CF, Naqvi S, Breitenbach J, Sandmann G, Christou P, Capell T (2008) Combinatorial genetic transformation generates a library of metabolic phenotypes for the carotenoid pathway in maize. ProcNatl Acad SciUS A 105: 18232-18237

Pubmed: Author and Title
CrossRef: Author and Title
Google Scholar: Author Only Title Only Author and Title